DTIC.

BANK STABILITY ALGORITHM FOR NUMERICAL MODELING OF CHANNEL WIDTH ADJUSTMENT

by

Stephen E. Darby and Colin R. Thorne

Department of Geography
University of Nottingham
University Park
Nottingham, UK
NG7 2RD

Final Report

to

US Army Research, Development
and Standardization Group-UK
London
under
Contract No.
N6817194C9062
Project No.
R&D 7059-EN-01

June 1995

SUMMARY

Existing numerical models of river channel morphology are seriously limited in their application by their inability to account for bank erosion and changing channel width. Recent research has, however, now led to the development of a physically-based numerical model of river channel widening, in which changing channel width is accounted for by coupling fluvial bank erosion and mass-wasting algorithms with flow and sediment transport models (Darby, 1994; Darby and Thorne, In Review). Verification studies indicate that this new model is capable of predicting channel adjustments well, qualitatively, but widening rates are seriously under-predicted by the new model (Darby *et al.*, In Review). This deficiency has focussed attention on the predictive ability of versions of the Osman and Thorne (1988) mass-wasting algorithm further developed by Darby (1994) and currently employed in the Darby-Thorne numerical model. In particular, the Osman-Thorne-Darby analysis constrains the failure plane to pass through the toe of the bank, excluding the possibility of simulating secondary, upper bank failures. The Osman-Thorne-Darby analysis also excludes pore water pressure and hydrostatic confining pressure effects. These deficiencies have been addressed conceptually by Simon *et al.* (1991), but this approach was developed only for banks of simple geometry, and does not account for the effects of pore and confining pressures on the development of the incipient failure plane. In contrast, the Osman-Thorne-Darby analysis utilises a more complete, physically-based approach in predicting failure plane angle, and the approach is also based on a bank profile characteristic of natural eroding riverbanks.

In this report, a new bank stability analysis is developed which combines the advantages of the Osman-Thorne-Darby analysis with the advantages of the Simon *et al.* (1991) analysis, with the aim being to improve the predictive ability of the mass-wasting algorithm and, therefore, the predictive ability of the numerical channel widening model. The new analysis is applicable to steep, cohesive, non-layered riverbanks which fail along planar failure surfaces. The analysis is developed for banks with profiles characteristic of natural, eroding riverbanks. Failure plane angles are calculated using a physically-based approach; additionally the failure plane is not constrained to pass through the toe of the bank. Pore water and hydrostatic confining pressure effects are included in the analysis. Using the procedure developed by Darby (1994), the new analysis also is capable of predicting the probability of mass failure, as well as the overall factor of safety with respect to mass failure.

In order to test the predictive ability of the new analysis, a data set, comprising 51 individual mass-failures, is also herein compiled. The data set itself is in a spreadsheet format on a diskette supplied with this report. The new data set represents the first compilation of data suitable for testing the ability of bank stability analyses to predict

accurately the factor of safety and geometry of individual observed mass-failures. The data set has been used to compare the predictive abilities of 4 bank stability analyses: Lohnes and Handy (1968), Huang (1983), Osman and Thorne (1988) and the analysis developed in this report. Results indicate that the analysis developed in this report is the most successful of the tested analyses in predicting the stability of riverbanks with respect to mass failure. However, the new analysis still significantly over-predicts bank stability. Nevertheless, it is demonstrated that the new analysis provides significant improvements to predictions of bank stability when compared to the Osman and Thorne (1988) analysis. It is, therefore, likely that application of the new analysis developed herein in the Darby-Thorne numerical channel evolution model would result in improved quantitative predictions of channel adjustment. Implementation of the new bank stability analysis in the numerical channel morphology model is a topic of current research.

In the meantime, the new bank stability analysis may be used as a stand-alone tool to aid engineers in the design of stable channels. To this end, the new analysis has been developed as a computer program, which is supplied on disk with this report, together with supporting documentation. The computer program may be used to calculate the factor of safety or probability of failure of riverbanks of geometry specified by the user. The user must specify the geotechnical characteristics of the bank material and select whether or not to include pore water and/or confining pressure effects in the analysis. If the user does select either these options he or she must specify the ground water surface elevation and elevation of the surface water in the channel, respectively.

A particular feature of the computer program is that it may be used to determine the amounts of fluvial, particle-by-particle, erosion and bed degradation required to destabilize an initially stable bank to the point of failure. This feature will allow the computer program to be utilised as a design aid in a variety of stable channel design applications, such as determining minimum grade-control structure elevations required to prevent degradation initiating channel widening and instability or in estimating volumes of sediment supplied to the channel from fluvial erosion/bed degradation induced bank failures. The ability of the model to generate predictions of probability of failure will also allow the program to be used as a tool in reliability analyses (*e.g.* Johnson, 1992)

CONTENTS

1. Introduction 7

2. Objectives 10

3. Riverbank Stability Analysis 10

- 3.1 Stability Analysis 13
- 3.2 Pore Water Pressure 15
- 3.3 Hydrostatic Confining Pressure 17
- 3.4 Failure Plane Angle 26
- 3.5 Location of Most Critical Failure Surface 29
- 3.6 Geometries of Mass Failures 30
- 3.7 Probabilistic Bank Stability Analysis 31
- 3.8 Computational Procedure 36
- 3.9 Limitations of Analysis 37

4. Analysis of Predictive Ability of Selected Riverbank Stability Analyses 38

- 4.1 Selection of Bank Stability Analyses 38
- 4.2 Collation of Data 39
- 4.3 Assessment of Predictive Ability of Stability Analyses 41
  - 4.3.1 Factor of Safety Analysis 41
  - 4.3.2 Geometry of Incipient Failure Blocks 44
  - 4.3.3 Critical Geometry: Darby-Thorne Analysis 50

5. Summary and Conclusion 54

Acknowledgements 55

Appendixes

- Appendix I. References 56
- Appendix II. List of Symbols 58
- Appendix III. Bank Geometry Database Users Manual 60
- Appendix IV. Bank Stability Model Users Manual 63

LIST OF FIGURES

Figure 1 Sediment fluxes in the near bank zone (after Thorne and Osman, 1988) 8
Figure 2 Characteristic geometry of bank stability analysis 11
Figure 3 Characteristic geometry of natural, eroding riverbank 12
Figure 4 Bank stability analysis definition diagram 13
Figure 5 Impact of surface and ground water on pore pressure at a point on the incipient failure plane 16
Figure 6 Solutions for pore water pressure 17
Figure 7 Influence of hydrostatic confining pressure on bank stability in absence of ground water 20
Figure 8 Solutions for hydrostatic confining pressure 24
Figure 9 Computational procedure used in bank stability analysis 30
Figure 10 Computational procedure used in probabilistic bank stability analysis (after Darby, 1994) 35
Figure 11 Example of over-laid cross-section surveys used to estimate critical geometries of mass-failures 40
Figure 12 Comparison of frequencies of occurrence of predicted factors of safety with "observed" factor of safety for (A) Lohnes and Handy (1968), (B) Huang (1983), (C) Osman and Thorne (1988), and (D) Darby-Thorne bank stability analyses 42
Figure 13 Comparison of predicted versus observed failure plane angle for (A) Lohnes-Handy, (B) Huang, (C) Osman-Thorne, and (D) Darby-Thorne bank stability analyses 46
Figure 14 Comparison of predicted versus observed failure block volume for (A) Lohnes-Handy, (B) Huang, (C) Osman-Thorne, and (D) Darby-Thorne bank stability analyses 47
Figure 15 Comparison of predicted versus observed failure block width for (A) Lohnes-Handy, (B) Huang, (C) Osman-Thorne, and (D) Darby-Thorne bank stability analyses 48
Figure 16 Predicted versus observed (A) Failure plane angles (B) Failure block volumes (C) Failure block widths and (D) Flood-plain widening increments obtained using the Darby-Thorne analysis for critical conditions 53
Figure AIV1 Definition diagram illustrating bank geometry parameters used in example applications 82

LIST OF TABLES

Table 1 Riverbank soil and geometry characteristics at varying scales (from Darby, 1994) 32

Table 2 Summary of characteristics of bank stability analyses selected for predictive comparison 39

Table 3 Summary of predictive abilities of selected bank stability analyses 43

Table 4 Summary of abilities of selected bank stability analyses to predict failure block geometry ("worst-case" conditions) 45

Table 5 Summary of calculated mean discrepancy ratio and absolute deviation of the discrepancy ratio for critical failure block geometry conditions using the Darby-Thorne bank stability analysis 51

Table AIV1 Example of format of UNITWEIG.DAT input data file 65

Table AIV2 Example of format of FRICTION.DAT input data file 66

Table AIV3 Example of format of COHESION.DAT input data file 67

Table AIV4 Example of format of SOILDATA.DAT input data file 68

Table AIV5 Summary of soil property parameters used in example applications 81

1. INTRODUCTION

Riverbank erosion and associated sedimentation and land loss hazards are a resource management problem of global significance. In the United States, an estimated 142,000 miles of stream bank are in need of erosion protection, with the cost of protecting US stream banks in 1981 about US$1 billion annually (U.S. Army Corps of Engineers, 1983). Not only may infrastructure located near destabilized river banks be threatened by accelerated bank erosion and land loss, but bank erosion often generates large quantities of fine-grained sediments that may pose a hazard to aquatic habitats as well as contributing to sedimentation problems downstream. For example, the U. S. Army Corps of Engineers (1983) study of the sediment budget in the Sacramento River showed that of the 11.5 million tons of total sediment inflow to the system, 6.8 million tons (59%) is derived from bank erosion. Such river bank instability is often triggered by human modifications, as well as by longer term natural modifications caused by climate change.

Recently, attempts to predict the land loss and bank sediment yield associated with riverbank instability and width adjustments (*e.g.* Lohnes, 1991; Darby and Thorne, 1992; 1994) have been made. These approaches have been based on estimating the failure geometry of banks that become unstable following bed degradation and/or direct fluvial erosion. However, the predictive ability and effectiveness of these approaches is limited by a number of unrealistic assumptions used in the analyses. First, the geometry of the eroding bank is usually specified in an unrealistic way. Most stability analyses specify the geometry of the bank profile using a single bank height and angle. In fact the geometry of natural eroding banks is more complex, due to processes of bed degradation or aggradation and direct lateral erosion acting to deform the bank face (Osman and Thorne, 1988). Most simple bank stability analyses also make unnecessary assumptions constraining the failure surface to pass through the toe of the bank. In fact, the failure surface may frequently not pass through the toe (Simon *et al.*, 1991). Finally, the influence of the surface and ground-water distributions on hydrostatic confining and pore-water pressures acting on the incipient failure block are also usually neglected (Simon *et al.*, 1991). There is a need to address these limitations in order to improve the predictive ability of methods of predicting land loss and bank sediment yield.

There is also a clear need to predict the response of rivers to changes in control variables and river engineering works in order to assess the influence of environmental and human-induced changes on channel form and also because channel form adjustments and lateral channel migration impact flood plain dwellers and users directly through erosion and sedimentation.

Studies of channel morphology have demonstrated the significance of the channel width as a dominant variable in controlling process-form interactions, probably through the

influence of width on secondary flow scaling (Yalin, 1971). This has resulted in the widespread use of the channel width as an independent or specified variable in the various channel morphology models, including numerical mobile-bed models such as HEC-6. HEC-6 is the preferred one-dimensional numerical model for water and sediment routing employed by Corps of Engineers personnel faced with real world problems. However, approaches which use the channel width as a constant, specified variable are in fact severely limited because channel changes in response to variations in flow or sediment regime are frequently dominated by transient width adjustments (Simon, 1992; Darby, 1994). Consequently, the application of existing numerical models of channel morphology, including HEC-6, is limited by their inability to account for bank erosion and changing channel width through time (Darby, 1994). The neglect of a widening predictor probably represents the most significant remaining limitation of HEC-6, and inclusion of such a predictor would represent a significant advance in the ability of HEC-6 to model stream channel erosion and sedimentation processes.

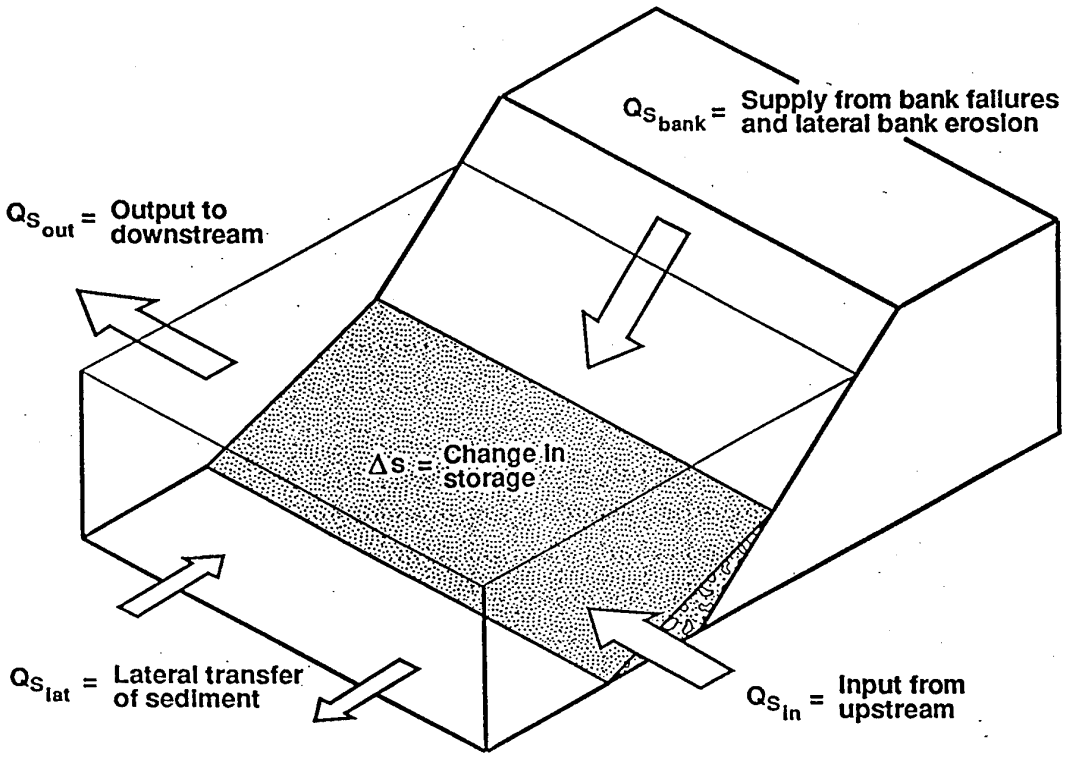

$$\Delta s = Qs_{in} - Qs_{out} \pm Qs_{lat} + Qs_{bank}$$

Figure 1 Sediment fluxes in the near bank zone (after Thorne and Osman, 1988)

Recently, advances in our ability to understand the processes and mechanisms of width adjustment in river channels have been made in research at the University of Nottingham, UK (Darby, 1994; Darby and Thorne, In Review; Darby *et al.*, In Review). This work has led to the development of a numerical model of channel morphology which includes adjustment of the channel width by coupling a quasi one-dimensional degradation/aggradation model with a bank stability algorithm in order to account for temporal trends in bank geometry and stability and the rate of retreat of the banks. This work has highlighted the importance of accurately modelling the fluxes of sediment entering and leaving the near bank zone (Figure 1) in order to model the rate of retreat or advance of the bank.

The research at Nottingham has shown that when riverbanks become unstable with respect to mass failure under gravity, it is the inflow of bank material that dominates the near bank sediment budget. Consequently, approaches based on predicting width by coupling bank stability models with bed morphology models must be able to predict accurately the onset of riverbank instability and the magnitude of the bank sediment flux, which is determined by the geometry of the mass failure. Indeed, under-predictions of widening rates in verification analyses of the Darby (1994) model were attributed primarily to the tendency of the existing (the Osman-Thorne-Darby) bank stability algorithm to under-predict failure block widths (Darby *et al.*, In Review). Development of a reliable bank stability algorithm is, therefore, also fundamental to the success of a widening predictor in a morphological model such as HEC-6. The development of an improved bank stability algorithm is also justified, therefore, through the potential improvement in the performance of HEC-6 that may be attained by incorporating the bank stability algorithm into the HEC-6 code.

One problem in evaluating objectively the predictive ability of riverbank stability analyses lies in the difficulties associated with measuring the geometries of eroding, unstable banks in the field. This has meant that there has up until now been a limited data set available to characterize natural unstable riverbanks at the point of failure. This has resulted in an inability to assess definitively the predictive ability of the wide range of existing bank stability analyses, leading to confusion and arbitrary selection of analyses by engineers faced with real world problems. It is apparent that collation of an improved database would aid greatly predictive comparisons of existing and new analyses of riverbank stability, helping to decide which stability analyses are most appropriate for analysing land loss, sediment yield impacts and channel adjustments resulting from bank erosion processes.

2. OBJECTIVES

To address directly the problems outlined in the preceding section, the objectives of this study are to:

1. Develop an improved analysis of the stability of natural, eroding, steep cohesive riverbanks which fail along planar surfaces;
2. Collate a set of data suitable for testing the new, and existing, analyses of bank stability;
3. Determine the predictive abilities of the new and existing analyses of riverbank stability using the data set obtained in objective (2);
4. Develop a computer model of bank stability based on the new bank stability analysis. This model will be developed bearing in mind the possibility of later incorporating the new analysis into the HEC-6 morphological model.

3. RIVERBANK STABILITY ANALYSIS

Over the years, a large number of slope stability models have been developed which have been applied to analyse the stability of eroding cohesive riverbanks. Reviews of these analyses have been made by Thorne (1982) and Huang (1983).

Traditionally, analyses of the stability of steep, cohesive eroding banks which fail along planar surfaces have been based on estimating the driving and resisting forces acting on incipient failure blocks with a relatively simple geometry (Figure 2), in which the failure block is described in terms of the overall bank height and a single bank angle (that is, the bank profile has only one surface). Examples of analyses based on geometries of this type include Lohnes and Handy (1968), Thorne *et al.* (1981) and Huang (1983). In these analyses, stability is modelled by defining a factor of safety (FS) as the ratio of resisting and driving forces acting on the incipient failure bock. Failure is predicted to occur when $FS < 1$, the dimensions of the failure being determined from the dimensions of the critical failure surface (Figure 2).

However, in practice, these previous analyses are limited by four major shortcomings when applied to natural, eroding riverbanks. First, the simple geometry used to characterize the dimensions of the incipient failure block shown in Figure 2 is inadequate to describe the geometry of natural eroding riverbanks (Osman and Thorne, 1988). This is because the profile of natural eroding riverbanks is deformed by combinations of bed degradation or aggradation, which influence the overall height of the bank, as well as direct lateral fluvial erosion, which acts to steepen the bank profile. These combinations of fluvial processes tend to result in a characteristic geometry of natural eroding riverbanks which may be more realistically illustrated by the schematic diagram shown in Figure 3. Second,

the failure plane is constrained to pass through the toe of the bank. This is unrealistic, since the most critical failure surface may intersect the bank profile at any point on the bank profile (Simon *et al.*, 1991). A third limitation is that the influences of soil pore water pressures and the hydrostatic confining pressure of surface water in the channel adjacent to the bank on the force distribution on the incipient failure block is either usually ignored, or characterized by an overly simplistic pore pressure ratio term (Simon *et al.*, 1991). Finally, the failure plane angle is not usually estimated using rigorous physically-based methods, but is instead frequently approximated as a function of bank angle and soil friction angle only.

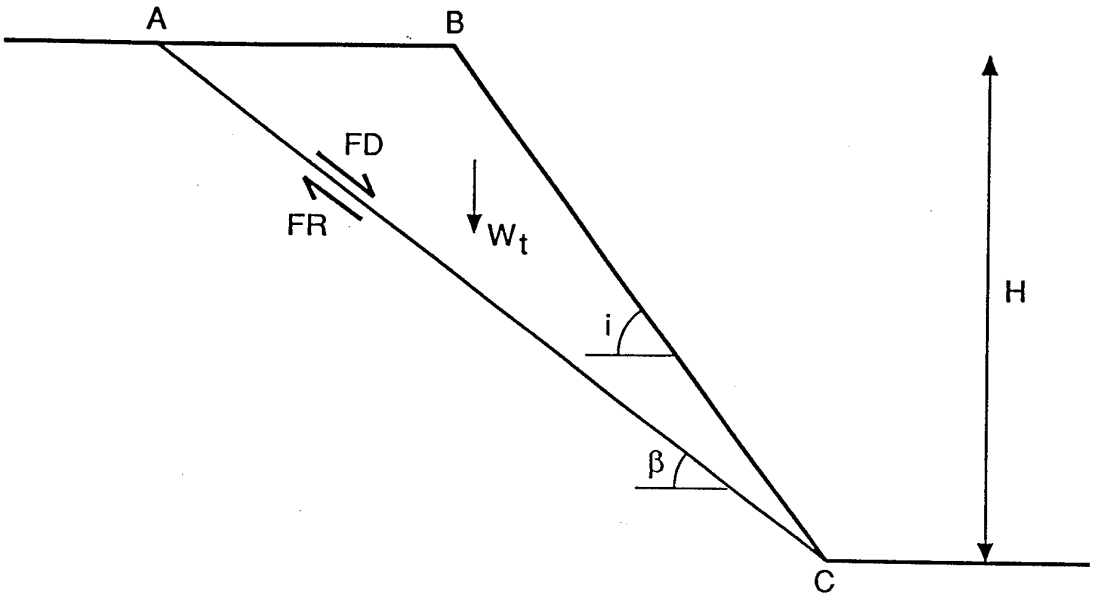

Figure 2 Characteristic geometry of simple bank stability analysis

Many of these limitations have individually, or in combination, been addressed in some more sophisticated analyses. Osman and Thorne (1988) derived an analysis of bank stability based on the more realistic geometry shown in Figure 3. They also calculated failure plane angle using physically-based techniques. However, pore water pressures and hydrostatic confining pressures were neglected in their analysis, and the failure plane was constrained to pass through the toe of the bank. Simon *et al.* (1991) developed a model of bank stability which did account for hydrostatic confining and pore water pressures, and in

which the failure plane was not constrained to pass through the toe. However, their model was based on the simple bank geometry of Figure 2, and failure plane angles were estimated using an overly-simplistic technique. Furthermore, there are some deficiencies in the Simon *et al.* analysis. Notably, this analysis does not account for the influence of dynamically interacting pore and surface waters on the pore water and hydrostatic pressure distributions. No model has yet been developed which attempts to address each of the limitations identified above in a single, unified analysis. The limitations associated with previous analyses should mean that the predictive ability of these approaches is not, therefore, as high as it could or should be.

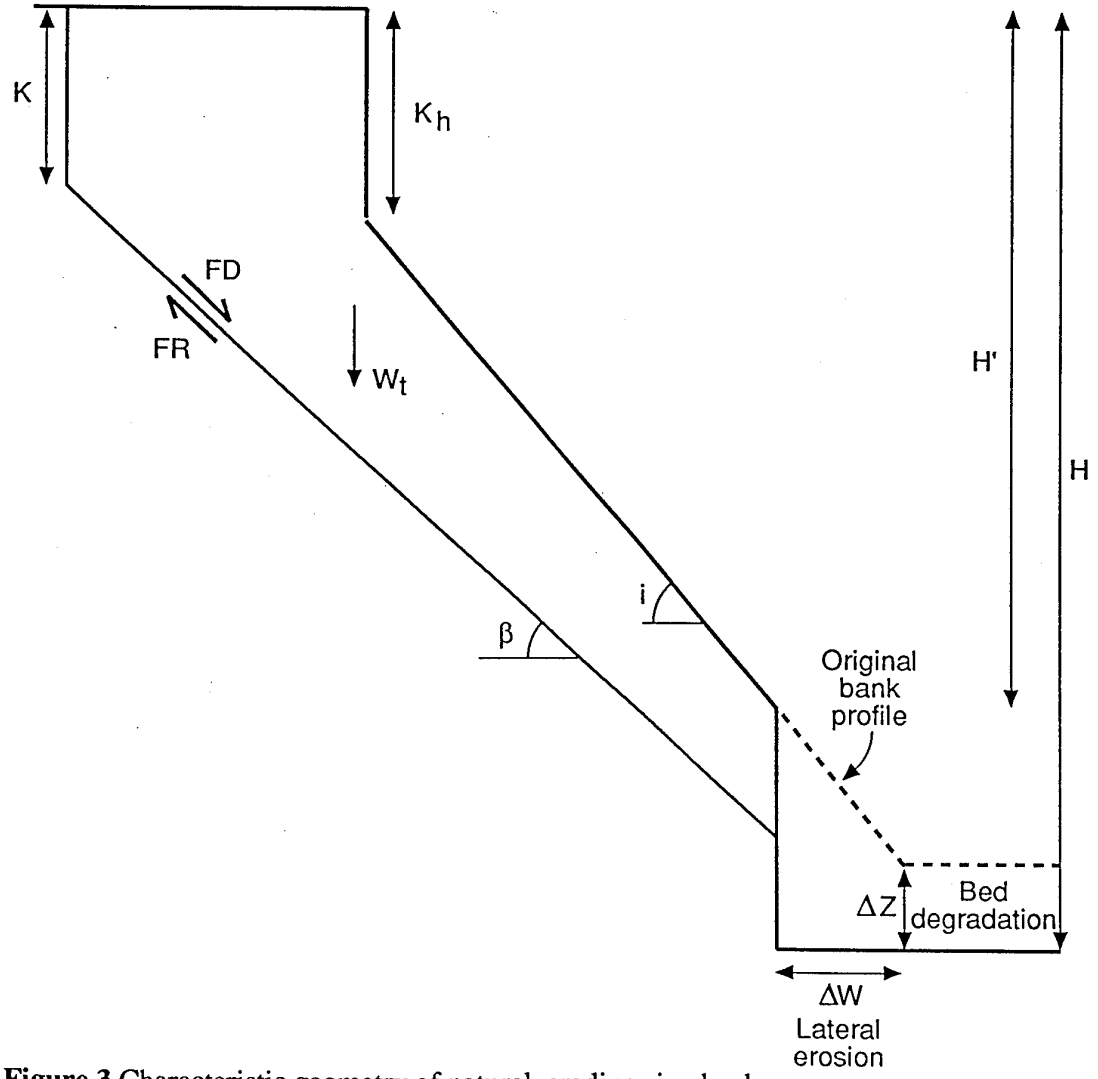

Figure 3 Characteristic geometry of natural, eroding riverbank

In response to the need to predict accurately the stability and geometry of incipient failure blocks along unstable river channels, a new analysis is developed herein in which

each of these limitations are addressed specifically. The development of the new model is now described.

3.1 Stability Analysis

The basic framework for the bank stability analysis is illustrated in Figure 4, which shows a bank with the more realistic geometry highlighted by Osman and Thorne (1988), but in which the failure block is subjected to pore water pressures, hydrostatic confining pressures and in which the failure plane is free to intersect the bank surface at any point along its profile. The task is to quantify each of the forces acting on the incipient failure block, including the effects of the pore water and hydrostatic confining pressures, while still allowing for the failure plane to intersect the bank profile at the most critical location. Additionally, the failure plane angle should be estimated using physically-based techniques.

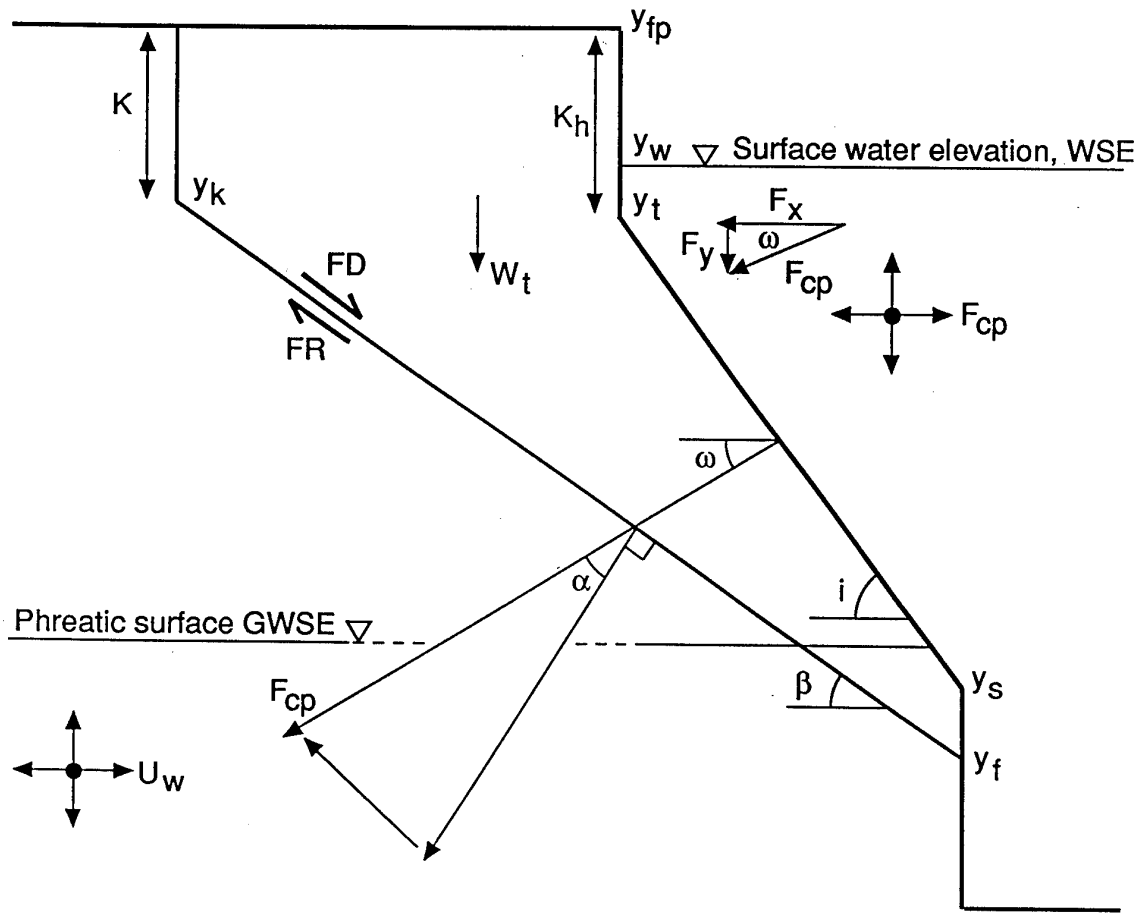

Figure 4 Bank stability analysis definition diagram

In order to obtain a solution, certain assumptions are required at the outset of the model derivation. These assumptions are that the bank is non-layered and that the effects of vegetation on bank stability may be excluded. It is assumed that the stability of the bank may be modelled using the factor of safety concept, where failures are detected once the ratio of the resisting and driving forces falls below unity. The factor of safety is defined by:

$$FS = \frac{FR}{FD} \tag{1}$$

where FS = factor of safety, FR = resultant resisting force on failure block (N) and FD = resultant driving force acting on failure block (N).

The resultant driving force acting on the incipient failure block is the resultant of the component of the weight of the failure block directed down the failure plane and the resultant of the hydrostatic confining pressure directed up the failure plane:

$$FD = W_t \sin\beta - F_{cp} \sin\alpha \tag{2}$$

where W_t = weight of failure block (Nm^{-2}), β = failure plane angle (degrees), F_{cp} = magnitude of the resultant hydrostatic confining pressure (Nm^{-2}) and α = angle between direction of resultant of the confining pressure and a normal to the failure plane (degrees).

The resisting forces acting on the failure block are a function of the cohesive and frictional resistance to sliding along the failure plane. Accounting for the effects of pore water and confining pressures, the resisting force is given by:

$$FR = c\,L + ((W_t - U_w)\cos\beta + F_{cp}\cos\alpha)\tan\phi \tag{3}$$

where L = length of failure plane (m), U_w = total pore water pressure acting on failure plane (Nm^{-2}), c = soil cohesion (Nm^{-2}) and ϕ = soil friction angle (degrees). By geometry:

$$W_t = \frac{\gamma}{2}\left(\frac{H^2 - K^2}{\tan\beta} - \frac{H'^2 - K_h^2}{\tan i}\right) \tag{4}$$

where γ = soil unit weight (Nm^{-3}), H = overall bank height (m), H' = uneroded bank height (m), K = tension crack depth (m), K_h = relic tension crack depth (m) and i = bank angle (degrees). The length of the failure plane is given by:

$$L = \frac{H - K}{\sin\beta} \tag{5}$$

Substituting (2) through (5) into (1) gives:

$$FS = \frac{\dfrac{C\,(H - K)}{\sin\beta} + \left(\left(\dfrac{\gamma}{2}\left(\dfrac{H^2 - K^2}{\tan\beta} - \dfrac{H'^2 - K_h{}^2}{\tan i}\right) - U_w\right)\cos\beta + F_{cp}\cos\alpha\right)\tan\phi}{\dfrac{\gamma}{2}\left(\dfrac{H^2 - K^2}{\tan\beta} - \dfrac{H'^2 - K_h{}^2}{\tan i}\right)\sin\beta - F_{cp}\sin\alpha}$$

To apply equation (6) it is, therefore, necessary to estimate the failure plane angle and pore water and confining pressure terms for given bank geometry, soil property and ground and surface water characteristics. Additionally, it is also necessary to determine the location of the most critical failure surface, in order to relax the constraint that the failure plane must pass through the toe of the bank. Each of these factors are now considered in turn.

3.2 Pore Water Pressure

In general, the pore water pressure exerted on the incipient failure plane at any point is given by:

$$u_w = \rho_w\, g\, (h_w + \varsigma) \qquad (7)$$

where u_w = pore water pressure at a point on the failure plane (Nm^{-2}), ρ_w = density of water (kgm^{-3}), g = gravitational acceleration (9.81 ms^{-2}), h_w = groundwater head (m) and ς = surface water surcharge (m) (Figure 5). Inclusion of the surface water surcharge term accounts for the influence of interacting pore and surface water pressures on the overall pore pressure distribution. So, the pore water pressure distribution along the incipient failure plane may be determined if the phreatic and surface water surfaces are known. To determine the total pore pressure acting on the length of the incipient failure plane, it is necessary to integrate (7) along the failure plane length, so that:

$$U_w = \sum_{0}^{x} u_w\, dx \qquad (8)$$

where U_w = total pore water pressure acting on the failure plane (Pa).

So, for any phreatic surface and surface water distributions, U_w may be estimated by expressing h_w and ς as functions of the phreatic and surface water elevations, the geometry of the incipient failure block, and x, the total failure block width (m). This can be done numerically for arbitrary distributions of ground and surface water distributions.

However, it is also possible to obtain numerical-analytical solutions for assumed special cases of bank and phreatic/surface water geometries. This is the approach adopted here. In this analysis, it is assumed that the phreatic surface is horizontal and parallel to the flood plain surface. For this case, it is possible to formulate U_w for a range of assumed ground water and surface water elevations. A total of 11 combinations are possible. These are illustrated in Figure 6 which, for clarity, also provides the various solutions for the total pore water pressure acting on the failure plane.

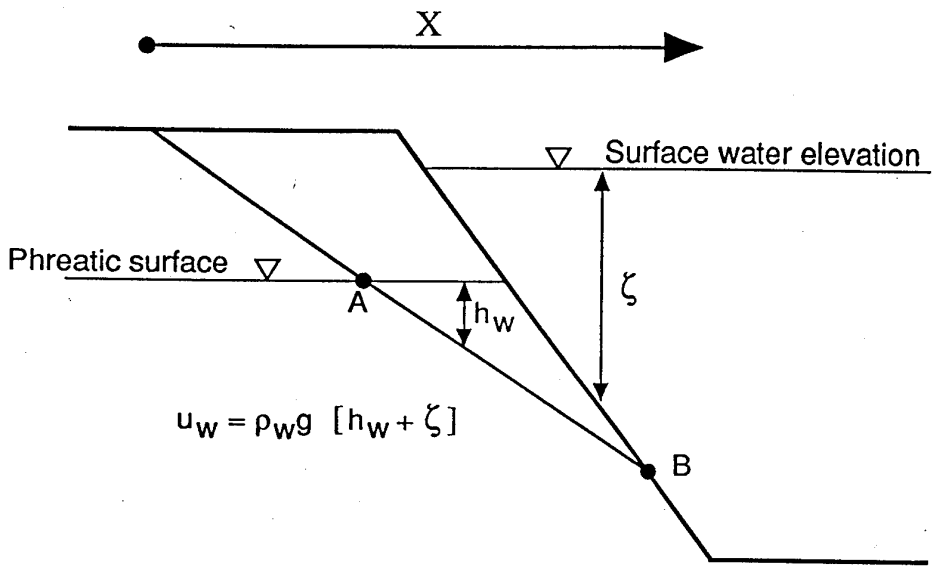

Figure 5 Impact of surface and ground water on pore pressure at a point on the incipient failure plane

It is important to stress that the solutions given in Figure 6 represent pore water pressures acting along the failure plane surface when the pore and surface waters are dynamically interacting. This is a departure from analyses which utilise pore pressure ratios to characterise the impact of pore water pressures on bank stability (*e.g.* Huang, 1983; Simon *et al.*, 1991). Such analyses are not able to account for the impacts of surface water surcharge on pore water pressure. It should be noted that the effects on bank stability of hydrostatic thrust exerted on a tension crack filled by precipitation are not considered here. Tension cracks filled by groundwater have no net hydrostatic thrusts exerted on them.

3.3 Hydrostatic Confining Pressure

Submerged incipient failure bocks may be subjected to a hydrostatic pressure exerted by the surface water in the channel. The aim of this section is to determine the

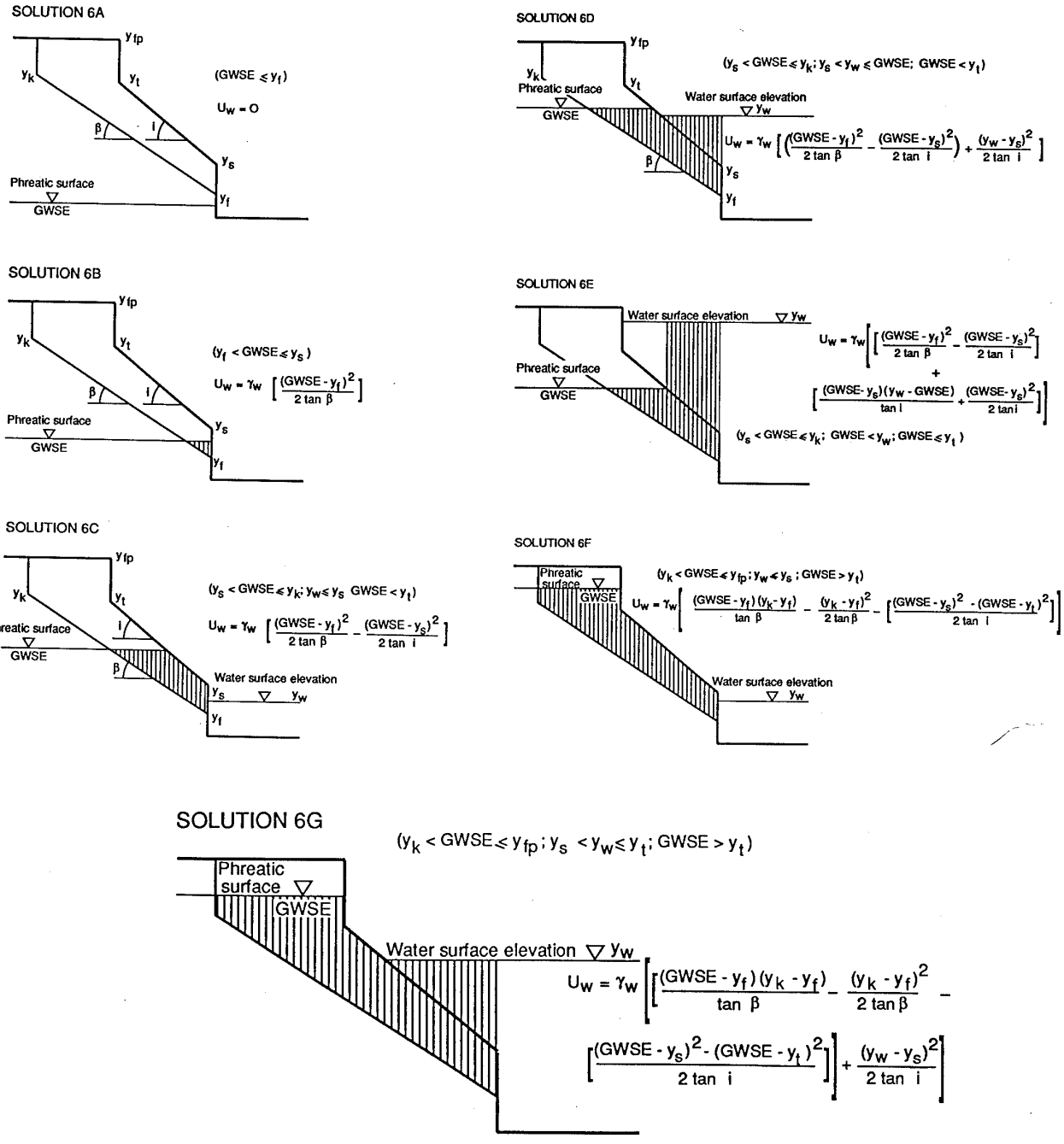

Figure 6 Solutions for pore water pressure

SOLUTION 6H

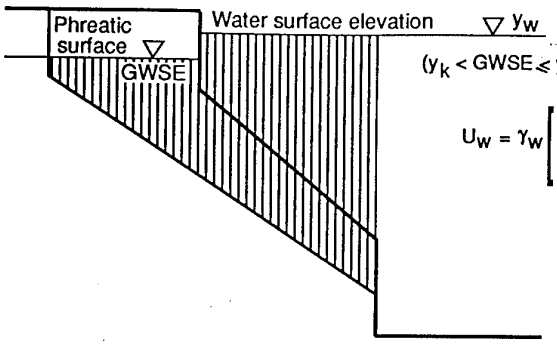

$(y_k < GWSE \leq y_{fp}; y_w > y_t; GWSE > y_t)$

$$U_w = \gamma_w \left[\left[\frac{(GWSE - y_f)(y_k - y_f)}{\tan \beta} - \frac{(y_k - y_f)^2}{2 \tan \beta} \right] - \left[\frac{(GWSE - y_s)^2 - (GWSE - y_t)^2}{2 \tan i} \right] + \left[\frac{(WSE - y_s)^2}{2 \tan i} - \frac{(y_w - y_t)^2}{2 \tan i} \right] \right]$$

SOLUTION 6I

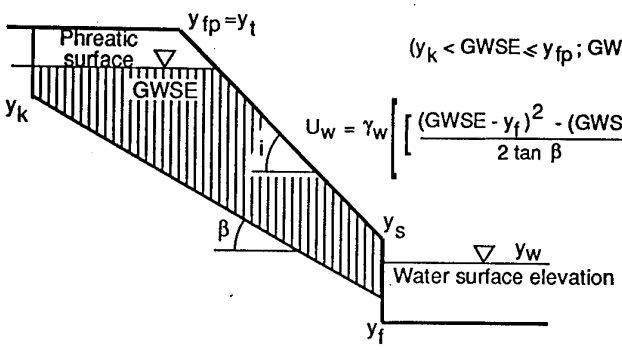

$(y_k < GWSE \leq y_{fp}; GWSE \leq y_t; y_s \geq y_w)$

$$U_w = \gamma_w \left[\left[\frac{(GWSE - y_f)^2 - (GWSE - y_k)^2}{2 \tan \beta} \right] - \left[\frac{(GWSE - y_s)^2}{2 \tan i} \right] \right]$$

SOLUTION 6J

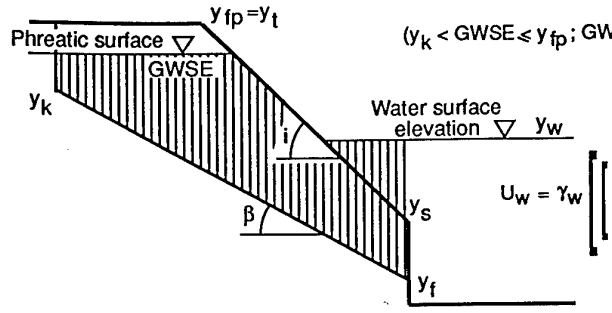

$(y_k < GWSE \leq y_{fp}; GWSE \leq y_t; y_s < y_w \leq y_t; GWSE > y_w)$

$$U_w = \gamma_w \left[\left[\left[\frac{(GWSE - y_f)^2 - (GWSE - y_k)^2}{2 \tan \beta} \right] - \left[\frac{(GWSE - y_s)^2}{2 \tan i} \right] \right] + \left[\frac{(y_w - y_s)^2}{2 \tan i} \right] \right]$$

SOLUTION 6K

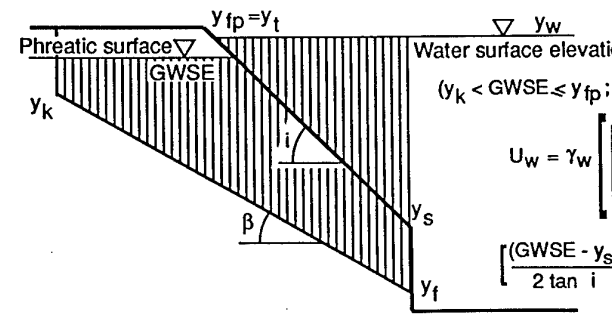

$(y_k < GWSE \leq y_{fp}; GWSE \leq y_t; y_w > GWSE)$

$$U_w = \gamma_w \left[\left[\left[\frac{(GWSE - y_f)^2 - (GWSE - y_k)^2}{2 \tan \beta} \right] - \left[\frac{(GWSE - y_s)^2}{2 \tan i} \right] \right] + \left[\frac{(WSE - y_f)^2 - (WSE - GWSE)^2}{2 \tan i} \right] \right]$$

Figure 6 Solutions for pore water pressure

hydrostatic confining pressure acting on submerged failure blocks with the geometry shown in Figure 3 for arbitrary surface water and phreatic surface elevations. A similar procedure was used by Simon *et al.* (1991), but they considered banks only with the simple geometry shown in Figure 2. They also did not account for interactions between the pore and surface waters in estimating the resultant confining pressure. These limitations are addressed here.

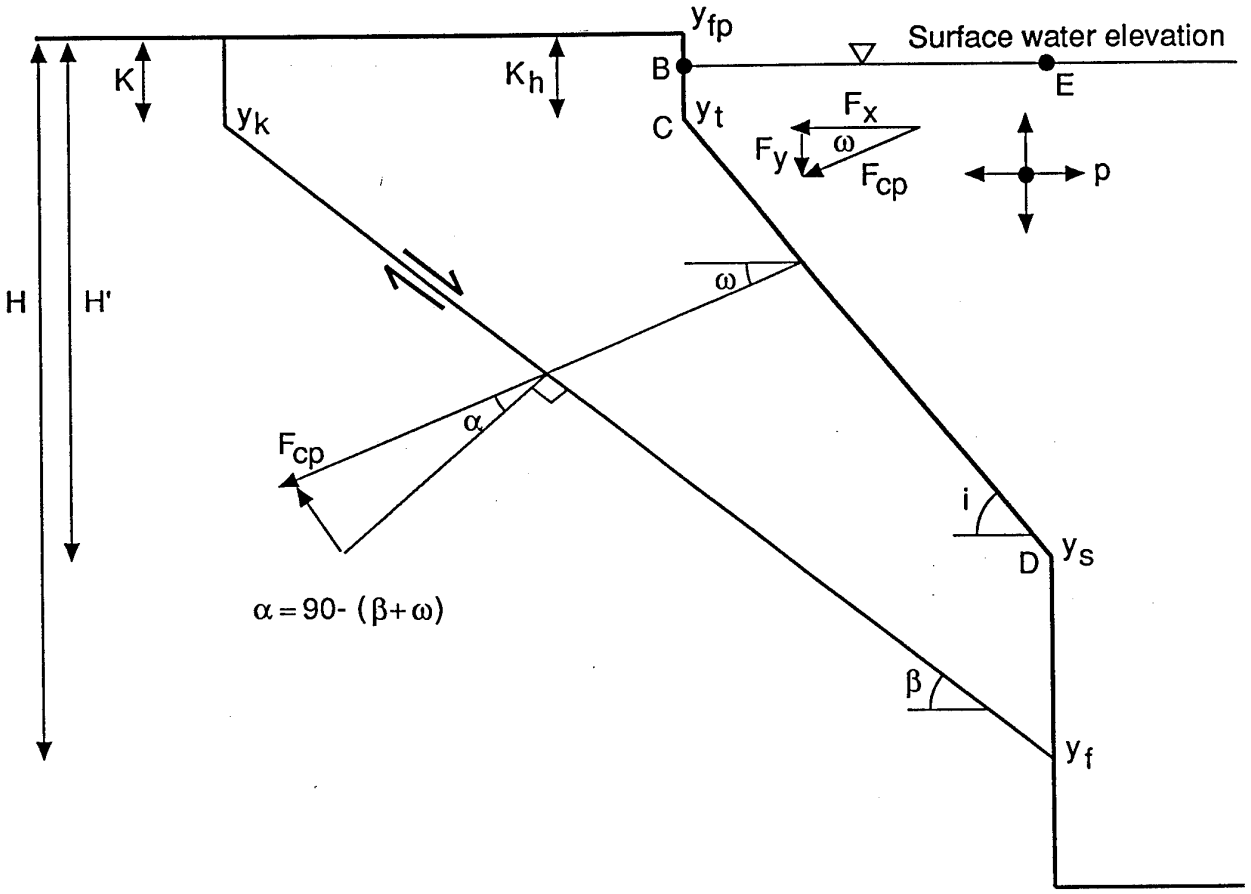

Figure 7 Influence of hydrostatic confining pressure on bank stability in absence of ground water

Consider Figure 7, in which the influence of the phreatic surface is neglected. The parameters of interest from the point of view of impact on bank stability (see Figure 4) are the magnitude of the resultant confining pressure, F_{cp}, and the angle, ω (degrees), at which

the resultant is directed through the bank surface, since these determine the components of F_{cp} acting on the incipient failure block, via the angle α. In fact the resultant hydrostatic confining pressure acting on an immersed, inclined, plane with complex geometry, such as that shown in Figure 7, can be estimated by resolving the forces acting horizontally and vertically on the immersed bank surface:

$$F_{cp} = \sqrt{F_x^2 + F_y^2} \tag{9}$$

The angle at which this resultant is directed through the bank surface is given by:

$$\tan \omega = \frac{F_y}{F_x} \tag{10}$$

where F_x = horizontal component of confining pressure (Nm^{-2}) and F_y = vertical component of confining pressure (Nm^{-2}). The total horizontal and vertical forces are given by the sum of all the forces acting on small, sub-elements of the bank surface:

$$F_x = \Sigma \partial F_x \tag{11}$$

$$F_y = \Sigma \partial F_y = W \tag{12}$$

where W = weight of the water above the bank surface (Nm^{-2}), that is the weight of the water contained in the volume BCDE in Figure 7. F_y is, therefore, given by:

$$F_y = W = \rho_w \, g \, (\text{Area BCDE}) \tag{13}$$

The precise value of Area BCDE depends on the surface water elevation, so the following possibilities are obtained:

$$F_y = \frac{\gamma_w}{2} \cot i \, [(y_w - y_s)^2 - (y_w - y_t)^2] \qquad (y_w > y_t) \tag{14}$$

$$F_y = \frac{\gamma_w}{2} \cot i \, (y_w - y_s)^2 \qquad (y_s < y_w \leq y_t) \tag{15}$$

$$F_y = 0 \qquad (y_w \leq y_s) \tag{16}$$

where γ_w = unit weight of the surface water (assumed to be 9810 Nm^{-3}) and y_f, y_s and y_t = elevations of points on the bank profile (m) (see Figure 7) and y_w = water surface elevation

(m). The value of F_x is given by the sum of all horizontal components acting on the bank face, so that:

$$F_x = F_{x1} + F_{x2} + F_{x3} \tag{17}$$

where F_{x1} = pressure force acting on projection of face AC (Nm^{-2}), F_{x2} = pressure force acting on projection of face CD (Nm^{-2}) and F_{x3} = pressure force acting on projection of face DF (Nm^{-2}). These terms are given by the following set of equations:

$$F_{x1} = \frac{\gamma_w}{2}(y_w - y_t)^3 \qquad (y_w > y_t) \tag{18}$$

$$F_{x1} = 0 \qquad (y_w \leq y_t) \tag{19}$$

$$F_{x2} = \frac{\gamma_w}{2}(y_w - y_s)^3 \qquad (y_w \leq y_t) \tag{20}$$

$$F_{x2} = \frac{\gamma_w}{2}(y_t - y_s)^3 \qquad (y_w > y_t) \tag{21}$$

$$F_{x3} = \frac{\gamma_w}{2}(y_s - y_f)^3 \qquad (y_w \geq y_s) \tag{22}$$

$$F_{x3} = \frac{\gamma_w}{2}(y_w - y_f)^3 \qquad (y_w < y_s) \tag{23}$$

these expressions can be substituted back into equations to obtain the following expressions:

$$F_{cp} = \sqrt{\left(\frac{\gamma_w}{2}(y_w - y_f)^3\right)^2 + \left(\frac{\gamma_w}{2}\cot i\,[(y_w - y_s)^2 - (y_w - y_t)^2]\right)^2} \tag{24}$$

$$\tan\omega = \frac{\cot i\,[(y_w - y_s)^2 - (y_w - y_t)^2]}{(y_w - y_f)^3} \qquad (y_w > y_t) \tag{25}$$

$$F_{cp} = \sqrt{\left(\frac{\gamma_w}{2}(y_w - y_f)^3\right)^2 + \left(\frac{\gamma_w}{2}\cot i\,(y_w - y_s)^2\right)^2} \tag{26}$$

$$\tan \omega = \frac{\cot i \, (y_w - y_s)^2}{(y_w - y_f)^3} \qquad (y_s \le y_w \le y_t) \qquad (27)$$

$$F_{cp} = \frac{\gamma_w}{2} (y_w - y_f)^3 \qquad (28)$$

$$\tan \omega = 0 \qquad (y_w < y_s) \qquad (29)$$

$$F_{cp} = 0 \qquad (30)$$

$$\tan \omega = 0 \qquad (y_w \le y_f) \qquad (31)$$

The angle, ω, at which the resultant of the confining pressure passes through the bank surface controls the angle, α (degrees), between the resultant of the confining pressure and the normal to the incipient failure plane (Figure 4), which influences the components of F_{cp} acting on the incipient failure block. By geometry, this angle is given by:

$$\alpha = 90 - (\beta + \omega) \qquad (32A)$$

$$\alpha = (i - \beta) \qquad (32B)$$

where equation (32B) is used only for submerged bank surfaces which are planar in shape (*i.e.* $H = H'$; $K_h = 0$).

It is possible to show that the line of action of the resultant of the confining pressure never intersects the tension crack (Figure 4), so long as the following condition is satisfied:

$$H - K > \frac{H}{3} - x \tan \omega \qquad (33)$$

This condition is not likely to be violated, since tension cracks depths rarely exceed half the overall bank height (Taylor, 1948). This is not a trivial result, for this guarantees that the line of action of the resultant of the confining pressure has the impact on the force distribution on the incipient failure block described by the F_{cp} terms in the factor of safety equation (6). No modification of this equation is, therefore, required to account for the influence of confining pressure on tension cracking.

The equations developed above apply only to the case when there is no phreatic surface present, or the phreatic surface is below the base of the incipient failure block. In all other instances, the pore and surface waters along the saturated portion of the bank surface

interact. Along this portion of the bank surface the hydrostatic pressure is exerted equally in all directions, so that the net resultant hydrostatic confining pressure is equal to zero. The resultant of the confining pressure must, therefore, be calculated only along the section of the submerged bank face between the levels of the surface and groundwater elevations (Figure 8). However, it is relatively simple to estimate the resultant hydrostatic confining pressures under these circumstances. All that is required is to replace y_f in equations (24 to 31) with the elevation of the phreatic surface and to revise the effective locations of y_s and y_t accordingly. In fact there are a total of 12 possible combinations of surface water elevation, bank geometry and phreatic surface elevation, with specific solutions for F_{cp}, ω and α in each case. These cases are, for clarity, summarized in Figure 8.

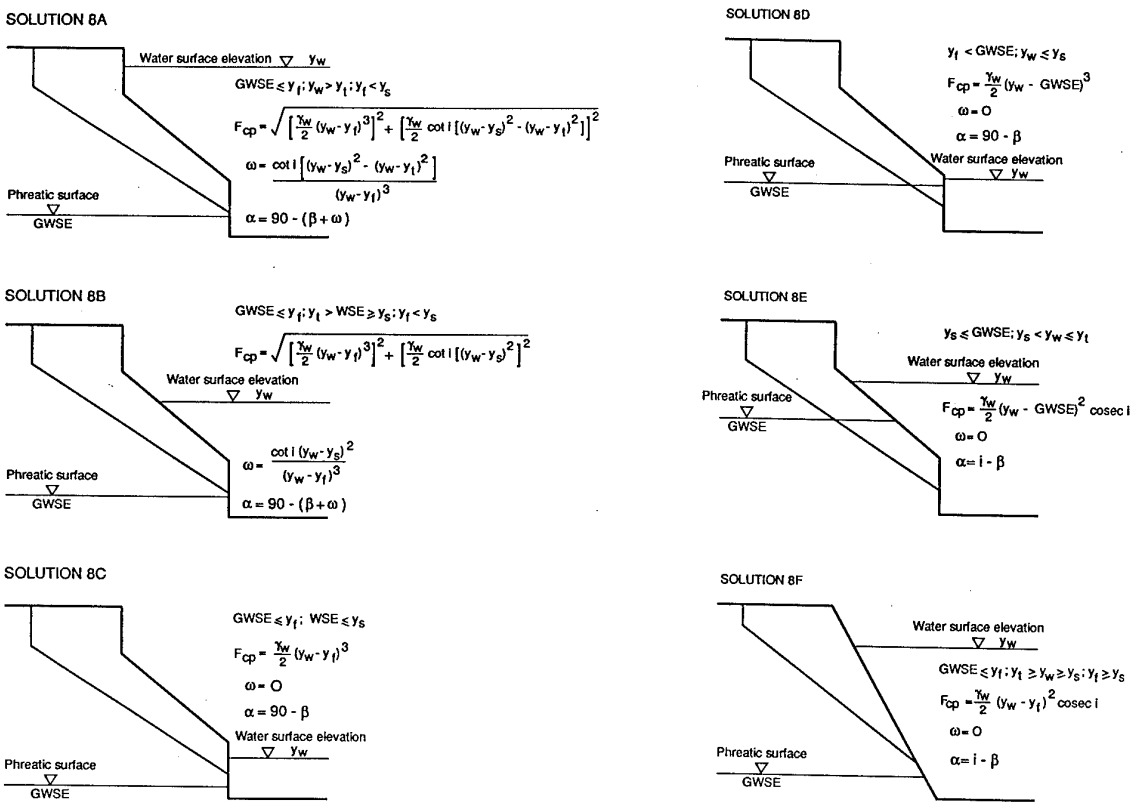

Figure 8 Solutions for hydrostatic confining pressure

SOLUTION 8G

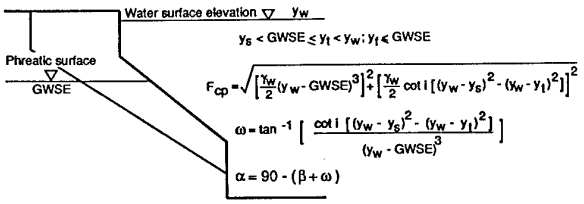

SOLUTION 8H

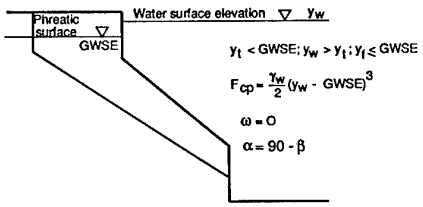

SOLUTION 8I

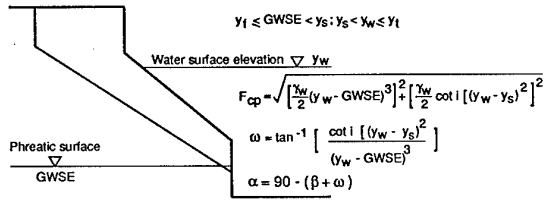

SOLUTION 8J

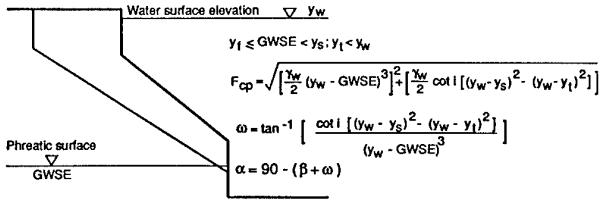

SOLUTION 8K

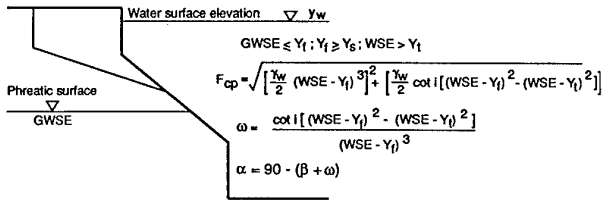

SOLUTION 8L

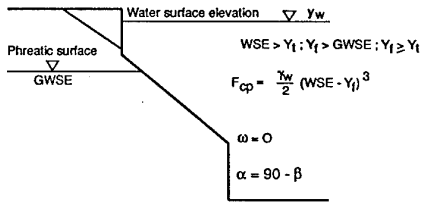

Figure 8 Solutions for hydrostatic confining pressure

In obtaining solutions for the confining pressure terms it is necessary to recognise the assumptions used in deriving the equations shown in Figure 8. The phreatic and water surfaces are assumed to be horizontal, and strictly speaking the equations are valid only for surface water with hydrostatic pressure distributions. Although this is a good approximation, even in many fluids undergoing motion, it should be recognised that pressure distributions close to the riverbanks may not always be hydrostatic, particularly in reaches with strong near bank secondary circulations with large vertical velocity components, as may be found close to the banks in curved reaches or at high flood flows (Darby and Thorne, 1993)

3.4 Failure Plane Angle

The failure plane angle, β, corresponds to that plane on which the cohesion, c, is fully developed at critical conditions (Taylor, 1948; Spangler and Handy, 1982; Osman and Thorne, 1988). This may be determined by equating the first derivative of the cohesion with respect to the failure plane angle in equation (6) to zero. In other words, the failure plane angle may be determined by estimating the angle, β, that satisfies the condition:

$$\frac{\partial c}{\partial \beta} = 0 \tag{34}$$

Rearranging (6) in terms of c gives the expression:

$$c = \frac{(W_t \sin^2\beta - F_{cp} \sin\alpha.\sin\beta) - [(W_t - U_w)\cos\beta.\sin\beta.\tan\phi + F_{cp} \cos\alpha.\sin\beta.\tan\phi]}{H - K}$$

where W_t, F_{cp}, α, and U_w are as defined previously. In fact, equation (35) is a more complex function of failure plane angle even than it first appears, since α and U_w are themselves functions of β. It is, therefore, necessary to rearrange the expressions for these parameters obtained in the previous sections in terms of β prior to estimating the first derivative of (35) with respect to β in order to obtain the condition defined by (34)

Differentiating the rearranged version of (35) and equating the result to zero leads to the following general expression, satisfied only by the true value of β:

$$\frac{\partial c}{\partial \beta} = \left(\left(\left(\frac{\gamma}{2}(H - K)(-\sin^2\beta + \cos^2\beta)\right) - \left(\frac{\gamma (H'^2 - K_h^2)\cos\beta.\sin\beta}{\tan i.(H - K)}\right)\right) - \left(\frac{F_{cp} X}{H - K}\right)\right)$$
$$- \left(F_n + \frac{F_{cp} \tan\phi\, Y}{H - K}\right) = 0 \tag{36}$$

where:

$$X = -\cos\beta.\sin(-90 + \beta + \omega) - \sin\beta.\cos(-90 + \beta + \omega) \quad (37A)$$

$$X = -\cos(i - \beta).\sin\beta + \sin(i - \beta).\cos\beta \quad (37B)$$

$$Y = \cos\beta.\cos(-90 + \beta + \omega) - \sin\beta.\sin(-90 + \beta + \omega) \quad (38A)$$

$$Y = \cos\beta.\cos(i - \beta) + \sin\beta.\sin(i - \beta) \quad (38B)$$

where equations (37B) and (38B) are used only if equation (32B) was selected, and:

$$F_n = \frac{\partial((W_t - U_w)\cos\beta.\sin\beta.\tan\phi)}{\partial\beta} \quad \frac{1}{H - K} \quad (39)$$

It is apparent that the form of equation (36) depends on the pore water and hydrostatic confining pressure distributions acting on the incipient failure block. It is possible to show that, for the special case when $H = H'$ and when $K = K_h = F_{cp} = U_w = 0$, equation (36) yields:

$$\beta = \frac{i + \phi}{2} \quad (40)$$

This is in fact the basis for the common usage of this simplified equation in many previous analyses (*e.g.* Lohnes and Handy, 1968; Huang, 1983; Simon *et al.*, 1991). However, it will be clear that the combination of conditions that lead to the derivation of (40) will rarely be satisfied for natural riverbanks, so that analyses which employ (40) will have limited validity. Osman and Thorne (1988) solved for the failure plane angle using an approach based on (34), but they did not include pore water and hydrostatic confining pressure terms in their analysis, either for factor of safety or failure plane angle. The analysis developed herein, therefore, represents a much more complete and physically-based approach to prediction of failure plane angle than previous analyses.

To solve equation (36) for the failure plane angle requires an iterative solution, since it is necessary to formulate F_{cp} and U_w in terms of the failure plane angle, resulting in a complex set of expressions. The approach adopted here is to use the Newton-Raphson iteration scheme in which successive estimates of β are obtained using:

$$\beta = \beta_{i-1} - \frac{F(\beta_{i-1})}{F'(\beta_{i-1})} \quad (41)$$

where $F(\beta_{i-1})$ is given by equation (36) and the derivative of this (with respect to β) is given by:

$$F'(\beta_{i-1}) = \left(\left(-2\gamma\,(H - K)\,(\sin\beta.\cos\beta)\right) - \left(\frac{\gamma\,(H'^2 - K_h^2)\,(-\sin^2\beta + \cos^2\beta)}{\tan i.H - K}\right)\right) - \left(\frac{F_{cp}\,X'}{H - K}\right) - \left(F_n' + \frac{F_{cp}\tan\phi\,Y'}{H - K}\right) \quad (42)$$

where:

$$X' = 2.\sin\beta.\cos(-90 + \beta + \omega) - 2.\cos\beta.\cos(-90 + \beta + \omega) \quad (43A)$$

$$X' = -2\sin\beta.\sin(i - \beta) - 2\cos\beta.\cos(i - \beta) \quad (43B)$$

$$Y' = -2.\cos\beta.\sin(-90 + \beta + \omega) - 2.\sin\beta.\cos(-90 + \beta + \omega) \quad (44A)$$

$$Y' = 2\cos\beta.\sin(i - \beta) - 2\sin\beta.\cos(i - \beta) \quad (44B)$$

where equations (43B) and (44B) are used only if equation (32B) is selected and:

$$F_n' = \frac{\partial^2((W_t - U_w)\cos\beta.\sin\beta.\tan\phi)}{\partial\beta^2}\,\frac{1}{H - K} \quad (45)$$

An initial estimate of the failure plane angle is made using the approximation:

$$\beta_o = \frac{i + \phi}{2} \quad (46)$$

Convergence is obtained when equation (36) is satisfied within a small error tolerance (0.01). The Newton-Raphson algorithm is a robust numerical method, and convergence is obtained satisfactorily in nearly all cases. However, certain combinations of F_{cp}, U_w and bank geometry lead to instances where converge does not occur, or the scheme converges to values of failure plane angle which are either negative or which are greater than the bank angle. If the iteration scheme fails to converge to a realistic solution, failure plane angle is estimated using equation (46). Fortunately, in test cases undertaken as part of this study such instances have been found to be very rare and have been confined to very stable banks with failure surfaces at high elevations, and very large applied hydrostatic confining pressures. The fact that these convergence problems arise only on the most stable failure

surfaces, with factors of safety well above unity (zero probability of failure) means that this unavoidable numerical problem does not influence prediction of critical failure surfaces.

There are 11 possible solutions for the above equations since, as discussed previously, there are 11 possible solutions of the pore water pressure term, each of which is a distinct function of β. These solutions are not presented here for the sake of clarity, though each possibility is written into the source code of the computer model based on this analysis (Appendix IV). In any case, each of the parameters in these equations have been presented in other forms in the preceding sections.

3.5 Location of Most Critical Failure Surface

The location of the most critical failure surface is predicted using an iterative search scheme based on that presented by Simon *et al.* (1991). They stress that this modification represents an important departure from conventional analyses of planar failures. In particular, this approach relaxes the assumption used in previous analyses (*e.g.* Lohnes and Handy, 1968; Osman and Thorne, 1988) that the failure plane must pass through the toe of the bank. This is important, as there is ample empirical evidence to indicate that mass failures can occur well above the bank toe (Thorne *et al.*, 1981; Simon and Hupp, 1986; Appendix III this report).

The basis of the computational scheme involves repeated calculation of the factor of safety at a number of different locations of the intersection of the failure plane with the bank surface. The most critical failure surface is discriminated by identifying the minimum predicted factor of safety. The computational procedure is illustrated in Figure 9. First, the search procedure divides the bank profile into 20 equal increments of bank height and projects these to the bank surface. Then, for each of these points the dimensions of the incipient failure block are determined by projecting a potential failure plane (at angle β, determined using the methods described above) to the flood plain surface. It is important to stress that, unlike the analysis adopted by Simon *et al.* (1991), β is allowed to vary and is calculated separately for each projected failure plane. Pore water and hydrostatic confining pressures and the factor of safety are then all estimated using the procedures presented in the preceding sections. The minimum factor of safety for the initial 20 points is then located.

If the minimum predicted factor of safety is greater than unity, or maximum predicted probability of failure (see below) is equal to zero it is assumed that the bank is stable with respect to mass failure. Otherwise a second search procedure is used to locate the most critical surface with greater precision (Figure 9). In this second search, the vertical bank height between the points immediately above and below the point at which the most critical surface located in the first search was identified, is divided into a further 20 equal

sub-increments. If the most critical failure plane identified in the first search is located at the bank toe, then the original increment between the bank toe and the first point above the toe is divided into 20 sub-increments. Computations are then repeated with the most critical failure surface located at the sub-point corresponding to minimum calculated factor of safety.

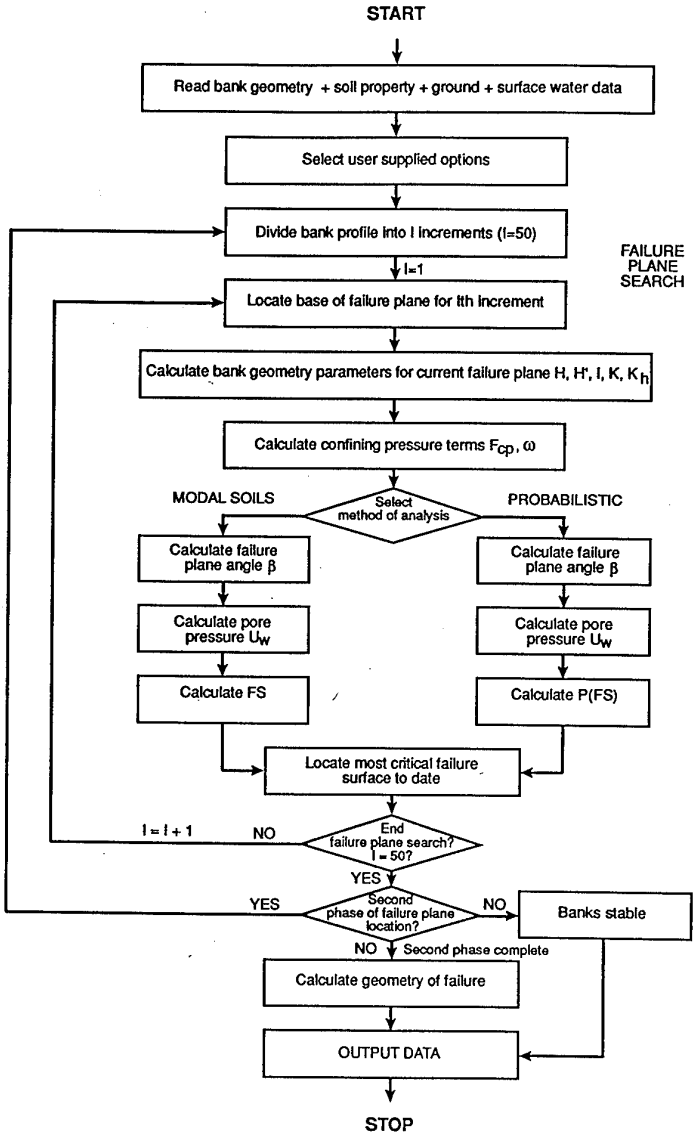

Figure 9 Computational procedure used in bank stability algorithm

3.6 Geometries of Mass Failures

If the factor of safety falls below the critical value, failure is predicted to occur. In calculating the geometry of the failure block, it is necessary to revise the effective bank geometry characteristics according to the location of the most critical failure surface, so that:

$$H = y_{fp} - y_f \tag{47}$$

$$H' = y_{fp} - y_s \qquad (y_f < y_s) \tag{48}$$

$$H' = y_{fp} - y_f \qquad (y_f \geq y_s) \tag{49}$$

$$K = y_{fp} - y_k \qquad (y_f < y_k) \tag{50}$$

$$K = \frac{y_{fp} - y_f}{2} \qquad (y_f \geq y_k) \tag{51}$$

$$K_h = y_{fp} - y_t \qquad (y_f < y_t) \tag{52}$$

$$K_h = 0 \qquad (y_f \geq y_t) \tag{53}$$

where y_{fp} = elevation of flood plain (m) and y_f = elevation of most critical failure surface (m). The geometry of the failure block is then given by:

$$BW = \frac{H - K}{\tan\beta} - \frac{H' - K_h}{\tan i} \tag{54}$$

$$x = \frac{H - K}{\tan\beta} \tag{55}$$

$$V = \frac{H^2 - K^2}{2\tan\beta} - \frac{H'^2 - K_h^2}{2\tan i} \tag{56}$$

where BW = flood plain widening increment (m), x = total failure block width (m) and V = volume of failure block per unit reach length (m^3m^{-1}).

3.7 Probabilistic Bank Stability Analysis

In modelling channel evolution through coupling bank stability analyses with numerical aggradation-degradation models, estimates of the total volumetric inflow of sediment from bank erosion along the length of modelled reaches are required as a loading term in the sediment continuity equation (Darby, 1994). However, 2-dimensional bank stability theories of the type described above provide estimates only of failure block dimensions per unit reach length. No information about the longitudinal extent of bank

failures is provided by these analyses. In the absence of information about the longitudinal extent of mass-failures the loading term in the sediment continuity equation is estimated using:

$$V_{ft} = \frac{V\,\Delta x}{\Delta T} \tag{57}$$

where V_{ft} = total volumetric bank material inflow flux due to mass failure (m^3s^{-1}), Δx = length of model reach (m) and ΔT = chosen time step over which the total volumetric inflow of bank materials is time averaged (s). Application of equation (57) assumes that once failure is detected at the computational node representing the model reach, banks along the entire length of the reach fail simultaneously. However, single mass failures are rarely observed over bank lengths of more than a few metres or tens of metres, even along the world's largest rivers. The spatial extent of natural mass failures will, therefore, be at least an order of magnitude smaller than the scale of mass failures modelled using this approach. Consequently, the bank material inflow rate determined using equation (57) will represent an unrealistically large maximum possible value which may be termed the "potential" bank material flux. Similarly, the flood plain widening increment and total failure block width values determined using equations (54) or (55) will also represent maximum "potential" values, BW^* and x^*.

Table 1 River bank soil and geometry characteristics at varying scales (from Darby, 1994)

SCALE	LENGTH (km)	SOILS	GEOMETRY
Micro (Single Failure)	< 0.05	Homogeneous (Low Variability)	Uniform
Meso (River Reach)	0.1 - 10	Heterogeneous	Uniform (Low Variability)
Macro (River Basin)	> 10	Heterogeneous	Non-Uniform

The problem appears to lie in mis-application of 2-dimensional bank stability theories, designed to predict the stability of relatively small lengths of bank in which the geometrical and geotechnical properties controlling the stability of the bank can reasonably be considered uniform (Table 1). Determination of the reach-scale sediment loading term requires application of the bank stability theory over a much larger spatial extent in which the geotechnical, if not the geometrical, properties cannot be expected to be uniform (Table 1). It follows that it is possible to obtain more realistic predictions of reach-scale stability

with respect to mass failure and reach-scale volumetric influx of bank materials by putting the deterministic bank stability theories outlined in the preceding sections into a probabilistic framework, so that the influence of statistical soil property variations along the reach on the factor of safety can be taken into account. By extension, the length of reach that is unstable with respect to mass failure may be equated to the estimated probability of failure. This approach allows the variability in geotechnical properties, assumed to control the micro-scale variation of stability along the reach, to be coupled with the meso-scale geometry in order to more realistically model the influence of sub-grid scale controls on river bank stability and the response of the reach as a whole. The hypothesis that the observed variation in bank stability along a river reach is due entirely to spatial variation in the geotechnical characteristics of the bank materials implies that it is reasonable to assume that the reach-scale geometry is uniform. This is anyway required within the conceptual framework of a numerical model in which cross-sections are chosen to characterize the morphology of individual reaches.

The procedure for calculating the probability of failure is based on that of Huang (1983). In essence, probability distributions representing the soils properties are substituted for single valued soil property variables in the factor of safety equations. The first step is, therefore, to determine the frequency distributions for each of the soil properties: cohesion, friction angle and unit weight. It is possible to define these distributions by measurement (*e.g.* Simon, 1989). By dividing each continuous frequency distribution into discrete classes, it is possible to define a finite number of combinations of soil properties, with representative values of each of the soil properties for each class. Each of these combinations, together with the reach-scale geometry, may be directly applied in the bank stability theories to determine the factor of safety for that individual combination of soil properties.The probability of occurrence of that predicted factor of safety, P(FS) is equated to the probability of occurrence of the soil property combination that gives rise to that particular factor of safety, given the constraints of the specified bank geometry:

$$P(FS)_{ijk} = P(c)_i * P(\phi)_j * P(\gamma)_k \qquad (58)$$

where $P(FS)_{ijk}$ = probability of the predicted factor of safety for an individual soil property combination, $P(c)_i$ = probability of the cohesion being in the class represented by the value c_i, and $P(\phi)_j$ and $P(\gamma)_k$ = probabilities of the friction angle and soil unit weight being represented by the values ϕ_j and γ_k, respectively. If the factor of safety calculated for a specific soil property combination is less than unity, failure is predicted for that combination. If failure is predicted, the probability given by equation (58) is stored while computations proceed through all the other possible combinations of soil properties. The probability of the overall factor of safety being less than unity is found from the sum of all

previously calculated probabilities corresponding to individual factors of safety of less than unity:

$$\mathrm{RP}(FS<1) = \sum_{i=1}^{i=i} \mathrm{P}(FS<1) \tag{59}$$

where RP(FS<1) = reach-scale probability of failure and P(FS<1) = probability of an individual factor of safety being less than unity.

Since the probability of failure is assumed equal to the fraction of the reach that fails, the "potential" bank flux and flood plain retreat increments determined from equations (54 to 56) can be modified to give the more realistic values:

$$V_m = \mathrm{RP}(FS<1)\ V \tag{60}$$

$$BW = \mathrm{RP}(FS<1)\ BW^* \tag{61}$$

$$x = \mathrm{RP}(FS<1)x^* \tag{62}$$

where V_m = total mass failure bank material influx per unit length of reach (m^2s^{-1}) and BW and x = reach-averaged flood plain widening increment and reach-averaged total failure block widths, respectively (m).

Following failure, the bank geometry is re-calculated using a reach-averaged updating scheme, so that a uniform reach-scale geometry is maintained at each computational node. For planar failures, bank geometry is updated using:

$$H = H \tag{63}$$

$$H' = (H'\ (1\text{-}\mathrm{RP}(FS<1)) + (H\ \mathrm{RP}(FS<1)) \tag{64}$$

$$K = (K\ (1\text{-}\mathrm{RP}(FS<1)) \tag{65}$$

$$K_h = (K_h\ (1\text{-}\mathrm{RP}(FS<1)) \tag{66}$$

$$i = (i\ (1\text{-}\mathrm{RP}(FS<1)) + (\beta\ \mathrm{RP}(FS<1)) \tag{67}$$

The computational procedure used to calculate the probability of failure and update the bank geometry is summarized in Figure 10. It will be noted that the implementation of the search for the most critical failure plane is similar to that employed in the non-probabilistic

approach, except that the most critical failure plane corresponds to the failure plane with the highest predicted probability of failure.

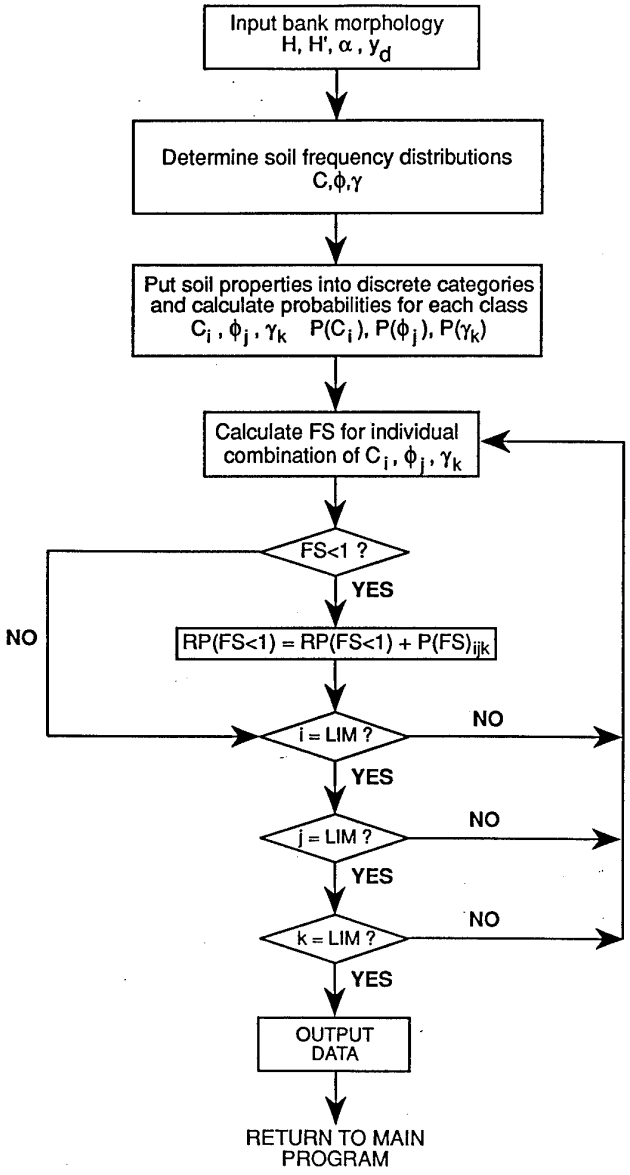

Figure 10 Computational procedure used in probabilistic bank stability analysis (after Darby, 1994)

The probabilistic approach does not require any assumptions to be made concerning the frequency distributions of the alluvial soils properties. In fact, these distributions may be determined by repeated measurements of soil properties in the field over the scale of the river reach (*e.g.* Simon, 1989). In effect, the new approach takes account of observed

variations in soil properties deterministically, emphasizing that the method is not a stochastic method of predicting the stability of river banks. The probabilistic approach may also, therefore, be used to assess the stability of heterogeneous bank materials, as well as the stability and land loss and sediment yield along lengths of riverbank.

The criterion for deciding to use the 2-dimensional or probabilistic analysis is somewhat arbitrary. If an at-a-site estimate is required, or if the soils are homogeneous, it is best to use the 2-dimensional analysis. Over larger space scales, the probabilistic analysis is preferred. In the computer model based on the analyses presented herein, the user is able to select either of the two analyses (Appendix IV).

3.8 Computational Procedure

The analysis developed in the preceding section has been developed in the form of a computer model which is supplied, with supporting documentation, with this report (Appendix IV). The computational procedures followed in applying these analyses in this model are now outlined and are illustrated in Figure 9.

First, the necessary bank geometry, ground and surface water and soil property data is supplied to the model. The user then selects a range of options which control the analysis. The bank profile is then divided into increments for the first sweep for the most critical failure plane. In re-positioning the base of the failure plane at each increment, the effective bank geometry for the failure plane is calculated using equations (47) to (53). The confining pressure terms are then calculated. The model then proceeds to the bank stability analyses, depending on which analysis the user specifies. In both cases, the computational scheme is broadly the same. The confining pressure terms, together with the bank geometry and soil property parameters, allow the failure plane angle to be estimated. The pore water pressure term is then estimated. Next the factor of safety, or probability of failure (depending on the selected analysis) are predicted. This procedure is repeated for all the selected failure plane locations, enabling the location of the most critical failure plane to be selected. If required, the second search sweep identifies the precise location of the most critical failure plane. The geometries of the simulated mass-failures (if detected) are then calculated. The output data is directed to files and computations stop.

The bank stability computer model supplied with this report may also be used to estimate the amount of fluvial erosion required to bring initially stable banks to the point of failure. By selecting the "critical geometry" analysis option of the computer program, the program automatically supplies increments of lateral fluvial erosion and bed degradation to the initially specified bank, until the point of failure is reached. The increments of lateral erosion and bed degradation applied to the bank are supplied in steps according to a user-specified ratio, $\frac{dW}{dZ}$, where dW is the increment of lateral fluvial (particle-by-particle)

erosion (m) and dW is the increment of bed degradation at the toe of the bank (m). In each step, 0.05m of degradation is automatically applied to the bank profile. The parameter $\frac{dW}{dZ}$, therefore, determines the magnitude of the of lateral erosion in each step. During the bed degradation, user-supplied water surface and ground water surface elevations are also lowered at appropriate rates.

The results file provides the user with the amount of degradation required to destabilize the banks, as well as estimates of the critical bank height and critical failure block magnitudes. This analysis will, therefore, be particularly useful for analysis of bank erosion and lateral channel stability in degrading systems. For example, the analysis could be used as a design tool to estimate elevations of grade control structures required to prevent knickpoint migration destabilising riverbanks and generating excessive channel widening.

3.9 Limitations of Analysis

It is appropriate to state the limitations of the new analysis. The analysis is applicable to steep, cohesive riverbanks which fail along planar surfaces. Banks are assumed to be non-layered and relatively homogeneous, though heterogeneous bank materials may be accounted for using the probabilistic bank stability analysis. The effects of vegetation and seepage effects are excluded. In calculating the soil pore water pressure, the phreatic surface is assumed to be horizontal and parallel to the flood plain surface. Surface water pressure distributions adjacent to the bank profile are assumed to be hydrostatic. The influence of hydrostatic thrust of (precipitation) water filled tension cracks is also excluded. Tension cracks are limited to maximum depths of no more than half the height of the bank.

It is important to take heed of these limitations during application of the computer program based on the riverbank stability analysis (Appendix IV), to ensure that computational instabilities do not arise. Known problems are now listed:

1. When using the probabilistic analysis, assigning a soil unit weight frequency distribution with low magnitudes of unit weight with non-zero probabilities of occurrence may lead to computed failure block weights less than the pore pressure exerted on the failure plane when the magnitude of the computed pore water pressure is also large. This can in turn can lead to negative values of factor of safety, which are difficult to analyse physically.
2. Low values of bank angle may, with large values of H' and small values of β, lead to computed failure block weights of less than zero, which is impossible. The computer model has been successfully applied on banks with a wide range of geometries and bank angles as low as 50 degrees. This value may be used as a guideline for the lower limit of bank angle that may be used in this analysis.

3. Values of tension crack depth greater than half the total bank height may lead to negative values of failure block weight, which is impossible. The computer program based on this analysis automatically constrains tension cracks so they do not exceed this maximum depth. This should be considered when interpreting analyses for which deeper cracks were specified by the user.

4. ANALYSIS OF PREDICTIVE ABILITY OF SELECTED RIVERBANK STABILITY ANALYSES

In this section, data obtained from natural stream channels undergoing erosion through mass-failures are used to test the predictive abilities of some selected riverbank stability analyses, including validation of the analysis developed in the preceding section. The comparison of the predictive abilities of the various analyses is used to elucidate which of the analyses is most suited to simulating the stability and geometry of cohesive stream banks undergoing planar mass-failures. The analysis should, therefore, be helpful in two regards. First, the analysis will aid river engineers in their selection of bank stability analyses for assessing channel stability. Second, the analysis should assist in selecting the most suitable mass-wasting algorithm for inclusion in numerical mobile-bed models, such as HEC-6, for development of mobile-width numerical modeling techniques.

4.1 Selection of Bank Stability Analyses

Even considering only the planar mechanism of mass-failure, a large number of bank stability analyses are available for consideration when selecting analyses to subject to assessment of predictive ability. At the outset of this study, it was planned to assess the predictive abilities of a wide range of analyses, including those developed by commercial software companies, academics, and other professionals. In this way, it was hoped that analyses in use by a whole spectrum of professionals would be subjected to an independent scrutiny of their predictive abilities. To the knowledge of the authors, no such independent scrutiny has been attempted previously.

However, this proved to be an overly optimistic goal. Despite contacting many individuals, academics, commercial software companies and private consultants, response to the authors requests to provide these analyses was generally poor. Many were not prepared to freely provide their codes, even solely for the purposes of this research. The resources of this project were not large enough to purchase these codes. The selected analyses are, therefore, restricted to stability analyses which are in the public domain and have been fully documented in the literature. Nevertheless, the results of the predictive comparison of the selected analyses will still be very useful, because the analyses tested are

by default well known and widely used. Furthermore, many commercially available codes which were not available for testing in this analysis are anyway based on analyses similar to those of Lohnes and Handy (1968) and Huang (1983), which are included in this predictive comparison.

In selecting bank stability analyses for assessment, a number of criteria were set. Selected analyses should be well known and widely used. It was hoped to obtain a range of complexity in the selected analyses, in order to allow assessment of whether or not increasing the physical basis and complexity of bank stability analyses is justified in terms of improved predictive ability. All the selected analyses should be applicable to planar failures in cohesive riverbanks. The analyses should be directly applicable to riverbank environments.

A total of 4 analyses were selected on this basis. These are the analyses of Lohnes and Handy (1968) (abbreviated to LH68), Huang (1983) (H83), Osman and Thorne (1988) (OT88) and the analysis developed in this study (Darby-Thorne) (DT94). The main features of these analyses have previously been described in the introduction, but are also summarized in Table 2. It can be seen that the listed order of these analyses roughly corresponds to an increasing level of complexity. It was hypothesized that the predictive abilities of the analyses would improve down the listed order.

Table 2 Summary of characteristics of bank stability analyses selected for predictive comparison

Analysis	Geometry	Failure Plane Analysis	Confining Pressure	Pore Water Pressure	Tension Crack
LH68	Simple	$\beta = \frac{i + \phi}{2}$	No	No	Yes
H83	Simple	$\beta = \frac{i + \phi}{2}$	No	Yes	Yes
OT88	"Natural"	Physically-Based	No	No	Yes
DT94	"Natural"	Physically-Based	Yes	Yes	Yes

4.2 Collation of Data

Few efforts to test rigorously the predictive ability of bank stability analyses have previously been made. In no small measure this is due to the difficulty in obtaining reliable

measurements of the critical geometry of mass-failures at the point of failure. Allied to the difficulty in obtaining the geometries of incipient failure blocks lies the problem of measuring the geotechnical soil properties of critical banks.

However, in the course of this research a reliable data set of 51 critical stream banks with corresponding geotechnical properties has now been compiled. This set of data represents a resource of considerable value. This data set has been provided in spreadsheet form on diskette, and is supported by Appendix III of this report.

Geometrical data relating to critical failure blocks were obtained in the following way. Repeated cross-section surveys along destabilized streams widening through bank failures have for a number of years now been made by United States Department of Agriculture personnel at frequent intervals along three streams in northern Mississippi: Hotophia Creek, Long Creek and Goodwin Creek. By overlaying plots of the sequences of the cross-section profiles obtained from the surveys, it was possible to estimate changes in bank geometry between surveys. In many instances these changes in cross-section geometry were characterised by mass failures (Figure 11). In this way, the geometries of mass failures were reconstructed using the survey data. When inspecting the over-laid profiles, care was taken to ensure that changes in geometry observed between surveys reflected only changes caused by mass failures. To ensure quality control, data were discarded if there was any doubt that an observed change in the bank profile did not represent a planar mass failure.

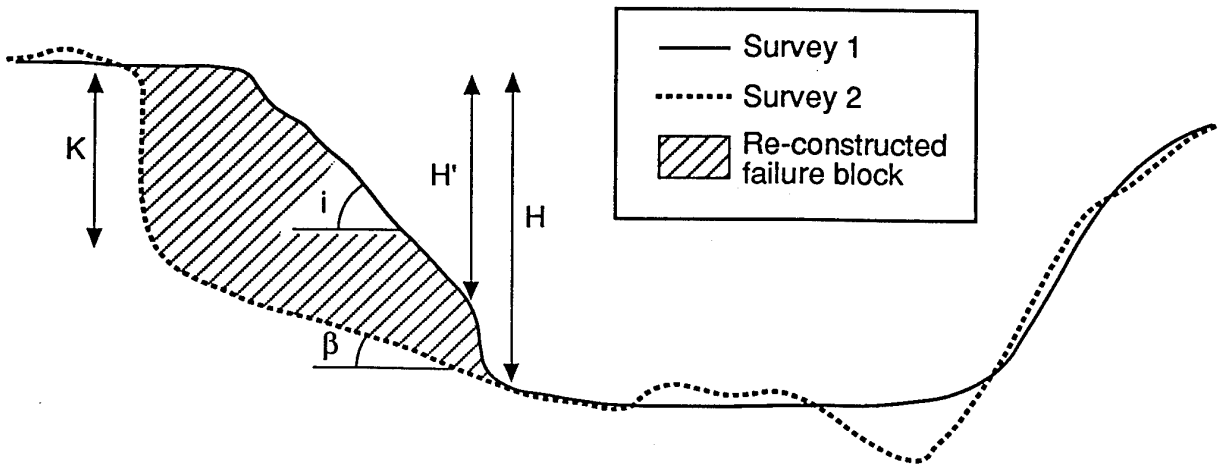

Figure 11 Example of over-laid cross-section surveys used to estimate critical geometries of mass-failures

The bank profile data so obtained were supplemented by measurements of the geotechnical properties of the bank materials. Direct measurements of soil properties have been made at sites along Long and Goodwin Creek by Thorne *et al.*, 1981. Full details of the measurement techniques and data so obtained are available in that report. It is assumed here that these measured properties, made only at a few sites, reflect soil characteristics throughout the period in which channel surveys were made (up to 1988). Since the stratigraphy and soil units at the Hotophia Creek sites were generally similar to those in the adjacent Long and Goodwin Creek watersheds, soil properties for the Hotophia Creek sites were estimated from the values determined at these nearby sites (Thorne *et al.*, 1981).

4.3 Assessment of Predictive Ability of Stability Analyses

Assessment of the predictive abilities of each of the tested analyses is made in two categories. First, the ability of each method to predict the overall stability of the bank with respect to mass failure under gravity is assessed by comparing predicted factors of safety to the critical factor of safety value of unity. Second, the ability of each analysis to predict the geometry of incipient failure blocks is assessed by comparing predicted failure block geometries with observed failure block geometries. These two aspects are now discussed.

4.3.1 Factor of Safety Analysis

Comparisons of predicted and observed factor of safety for each selected stability analysis were made in the following way. Observed critical bank geometries and geotechnical parameters at each of the 51 sites in the data set were used as input data in each of the 4 stability analyses, to obtain predicted factors of safety for each analysis at each of the 51 sites. These predicted values were then compared to "observed" values of factor of safety. For perfect agreement, predicted factors of safety should, at each site, be less than or equal to the "observed" critical value of unity. Assessment of the overall predictive ability of each analysis can, therefore, be made by comparing discrepancies between predicted and observed factor of safety.

In comparing predicted and observed factors of safety in this way, the reliability of the assessment of the relative predictive abilities of each analysis is dependent upon the quality of the data. While it is felt that the geometry of observed failures is described with high accuracy and reliability by this data set, no direct observations of the soil geotechnical parameters were made at the point of failure at any of the specific, individual, sites in the data set. Instead, geotechnical data were obtained from (reliable) measurements of soil properties at a few sites representative of the catchments in which the observed bank

failures were located. Moreover, these measurements where made when the soils were unsaturated and, therefore, represent "average", rather than the "worst case" conditions during which mass failures most likely occurred (Thorne *et al.*, 1981). "Worst case" estimates of the soil properties at each site were made by modifying arbitrarily the measured properties. Predictive comparisons were then made for both "average" and "worst case" conditions. In this way, although the precise values of the geotechnical data at the point of failure are not known for any of the sites, the range of values between the estimated worst case and average conditions almost certainly encompass the actual values encountered.

Figure 12 illustrates the results of the predictive comparison for each of the 4 selected analyses for the 51 sites combined, for both average and worst case soil properties. For comparative purposes, the "observed" critical factor of safety ($FS = 1$) is also illustrated. For an analysis to have been successful at any one site, in terms of predicting that the observed bank was unstable, the predicted factor of safety must be less than or equal to this critical value. For the purposes of this study, a reasonable tolerance level was specified, such that predictions of factor of safety were considered accurate if the predicted value of factor of safety was less than or equal to 1.2. This value is close enough to the critical case to be considered as successfully predicting a bank of unreliable stability.

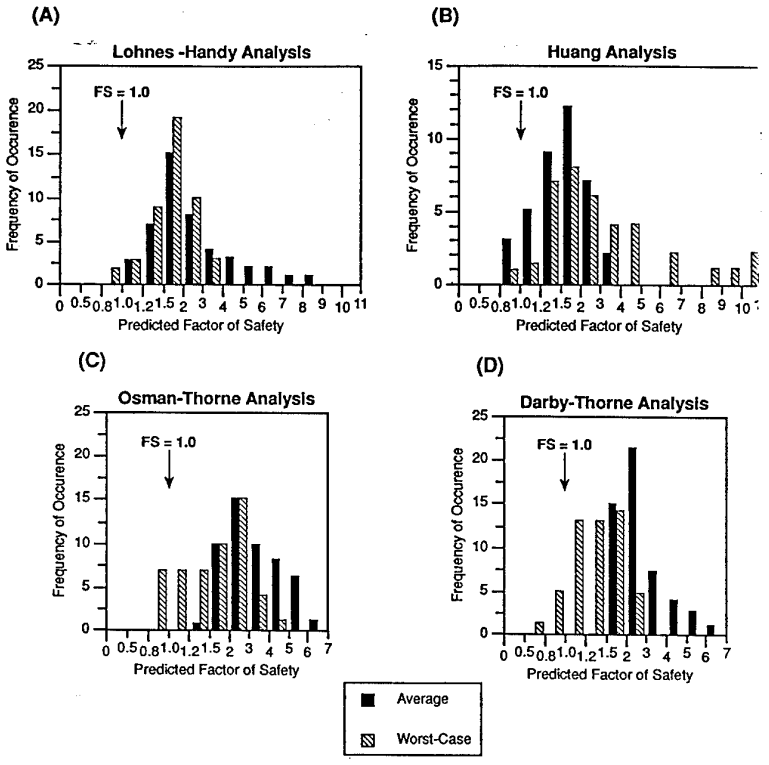

Figure 12 Comparison of frequencies of occurrence of predicted factor of safety and "observed" factor of safety for (A) Lohnes and Handy (1968), (B) Huang (1983), (C) Osman and Thorne (1988), and (D) Darby-Thorne bank stability analyses

Figure 12 shows that all 4 tested analyses tend to over-predict factor of safety. That is, all the tested analyses tend to predict more stable banks than actually observed. All of the analyses indicate correctly that factor of safety is predicted to decrease as soil properties tend to the "worst case" condition. However, there is considerable variation in both the degree to which each of the selected analyses over-predicts the factor of safety, and in the range of values predicted by each analysis (the degree of scatter of predicted values). Assuming that the "worst-case" data corresponds to the conditions when the banks were most likely to have failed (Thorne *et al.*, 1981), Figure 12 indicates that the most successful analysis in terms of having the highest number of sites predicted within the required range of $FS \leq 1.2$ ("worst-case" conditions) is the Darby-Thorne analysis (20 out of 51 sites fall in this category). The Darby-Thorne analysis is followed by the Osman-Thorne (14 out of the 51 sites), Lohnes-Handy (5 sites) and Huang (3 sites) analyses. This ranking of predictive ability is as expected and corresponds to the increasing level of complexity of the various analyses (Table 2).

To quantify an overall level of predictive ability of each of the bank stability analyses, comparisons of predicted versus observed factors of safety can be made in terms of the overall mean of the ratios of predicted to "observed" factors of safety for each of the 51 sites in the data set. This average value provides a simple, but reliable, quantitative estimate of the overall difference between predicted and observed values for each analysis. Assuming that the "observed" factor of safety is equal to one, the average discrepancies obtained for each analysis represent the mean of the 51 predicted factors of safety. These values are summarised in Table 3. This table confirms the impression of Figure 12 that the Darby-Thorne analysis is the most successful of the tested analyses, but even this analysis still somewhat over-predicts factor of safety.

Table 3 Summary of predictive abilities of selected bank stability analyses

Analysis	Mean Predicted Factor of Safety ("Average" soils)	Mean Predicted Factor of Safety ("Worst-case" soils)
Darby-Thorne (This report)	2.796	1.431
Osman and Thorne (1988)	3.200	1.816
Lohnes and Handy (1968)	2.690	1.828
Huang (1983)	3.676	3.257

4.3.2 Geometry of Incipient Failure Blocks

Although the stability of the banks with respect to mass failure is important in determining when the bank will collapse, predictions of the failure block geometry must also be correct if the amount of widening, volume of sediments delivered to the channel and morphology of the bank following mass-failure are also to be estimated accurately. Knowledge of these parameters is essential if quantitative predictions of the magnitudes of channel adjustments are required. In this regard the critical parameters are the failure plane angle, which determines the angle of the "new" bank surface following a mass-failure; the failure block volume, which determines the amount of bank material delivered to the channel; and the width of the failure block, which determines the magnitude of channel widening. The latter parameter is described here using both the total width of the failure block and the flood-plain widening increment (Figure 4).

Each of the 4 bank stability analyses tested in this study provide predictions of each of the parameters described above. Indeed it is the volume and shape of the incipient failure block that determines the diving and resisting forces which control the stability of the block with respect to mass-failure. Assessment of the ability of each bank stability analysis to predict the critical failure block geometry, therefore, provides important clues regarding the reasons for the success or failure of the various analyses to predict factor of safety. It is this aspect that is examined herein. To achieve this goal, predicted incipient failure block geometries are compared directly to the observed critical failure block geometries for each of the 4 selected bank stability analyses. Predictive ability is measured quantitatively using the mean of the discrepancy ratio (*Me*) and the absolute deviation of the discrepancy ratio (*Ad*):

$$Me = \frac{1}{n} \Sigma \frac{X_p}{X_o} \tag{68}$$

$$Ad = \frac{1}{n} \Sigma \left| \left(\frac{X_p}{X_o} - Me \right) \right| \tag{69}$$

where X_p = value of predicted parameter, X_o = value of observed parameter and n = number of data points in the data set. It is seen that the mean of the discrepancy ratio is defined as the arithmetic mean of the ratios of predicted to observed parameters for the data set as a whole, while the absolute deviation of the discrepancy ratio is a measure of scatter. It follows that perfect agreement between predicted and observed parameters occurs when $Me = 1$ and $Ad = 0$.

It should be noted that this approach is not a comparison of the ability of the various analyses to predict failure block geometry at the point of failure. This is because for any

predicted failure block geometry obtained using the observed data the predicted factor of safety may not be below the critical value, so that failure is not predicted to actually occur for that incipient failure block. To compare the ability of the models to predict the critical failure geometry parameters it would be necessary to use the models to determine the critical geometry and then compare these predicted values with the data. However, a comparison of each of the ability of each analysis to predict the critical geometry could not be attempted here because the Lohnes-Handy and Huang analyses are not implemented in this way. Instead the comparison of predictive abilities of each analysis is restricted to the case described in order to elucidate reasons for failure to predict accurately factor of safety. A full analysis of the ability of the Darby-Thorne analysis to predict failure block geometry at critical conditions is, however, provided in section 4.3.3.

Table 4 Summary of abilities of selected bank stability analyses to predict failure block geometry ("Worst-Case" conditions)

Model	Failure Plane Angle, β		Failure Block Volume, VB		Failure Block Width, X		Flood-Plain Widening, BW	
	Me	Ad	Me	Ad	Me	Ad	Me	Ad
LH68	1.237	0.386	0.391	0.259	0.703	0.311	0	0
Huang	1.281	1.309	1.030	0.736	1.249	0.482	2.053	1.464
OT88	0.561	0.129	2.586	1.417	1.714	0.551	3.478	1.919
DT94	0.867	0.359	1.982	1.372	1.349	0.627	2.951	1.848

Table 4 summarises calculated discrepancy ratios and absolute deviation parameters for the incipient failure block geometry parameters for each of the tested bank stability analyses for "worst-case" conditions. In addition, the scatter plots Figures 13 to 15 illustrate graphically the comparisons of predicted and observed values of failure plane angle, failure block volume and failure block width, again for "worst-case" conditions only.

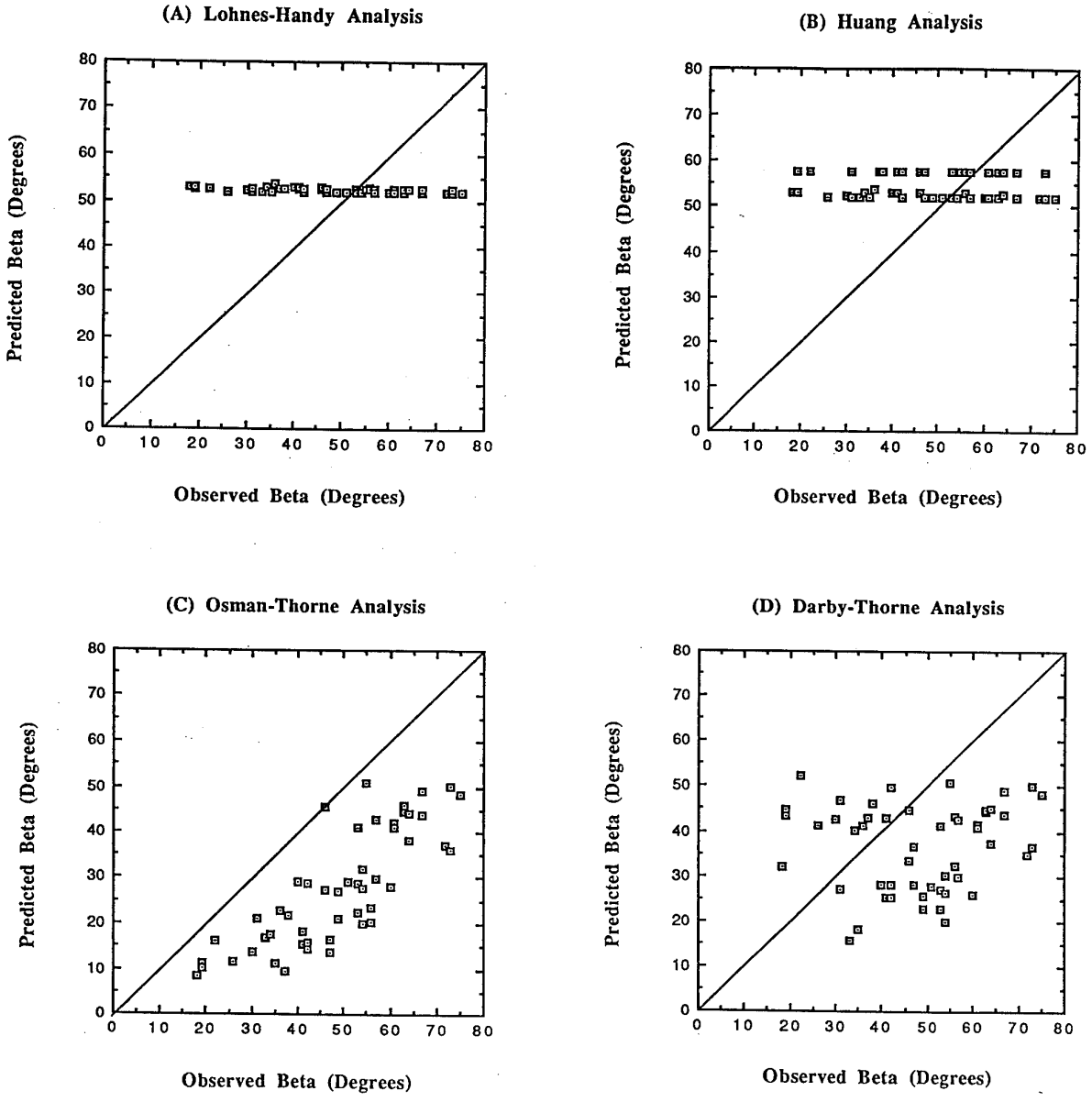

Figure 13 Comparison of predicted versus observed failure plane angle for (A) Lohnes-Handy, (B) Huang, (C) Osman-Thorne, and (D) Darby-Thorne bank stability analyses

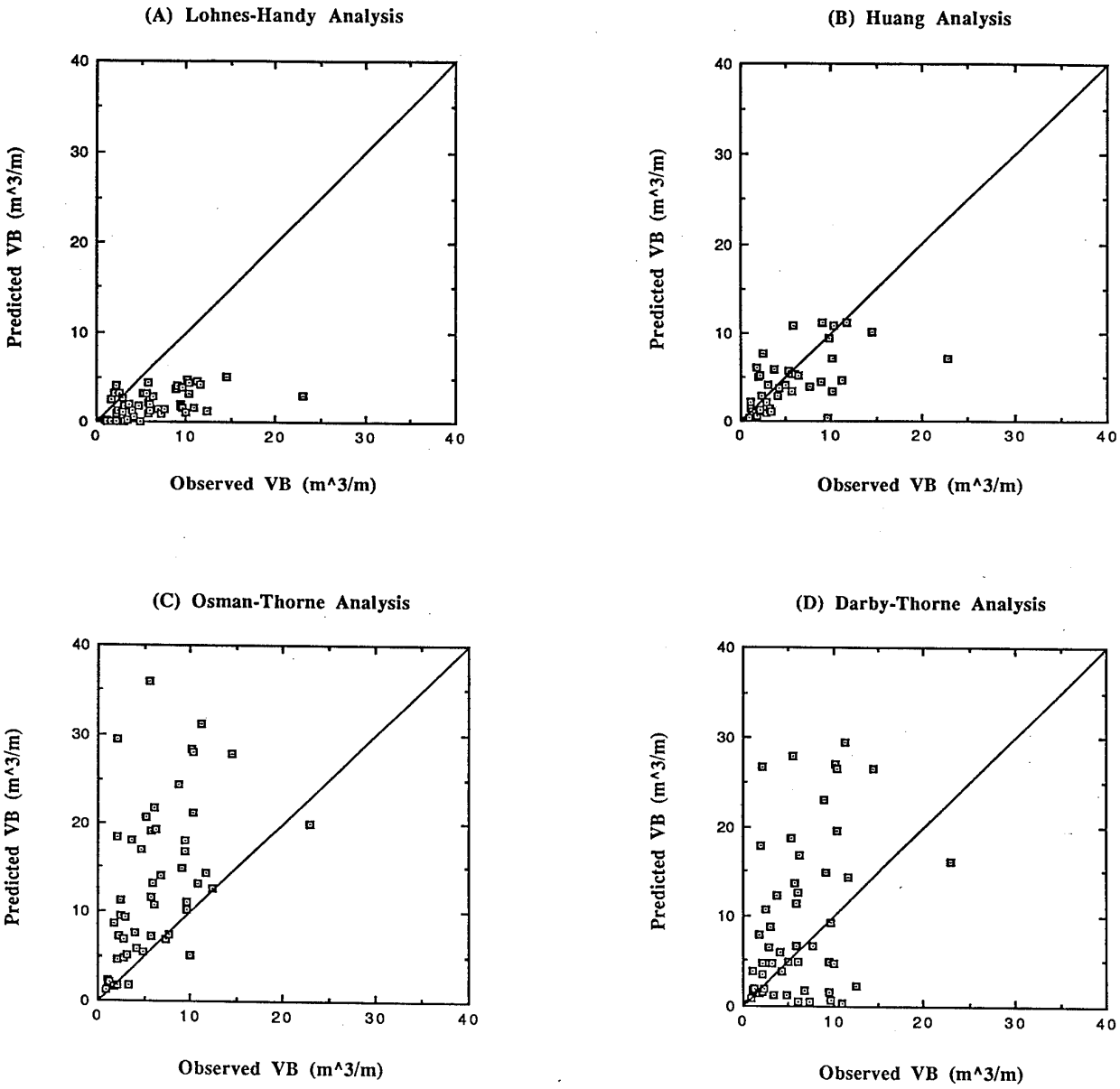

Figure 14 Comparison of predicted versus observed failure block volume for (A) Lohnes-Handy, (B) Huang, (C) Osman-Thorne, and (D) Darby-Thorne bank stability analyses

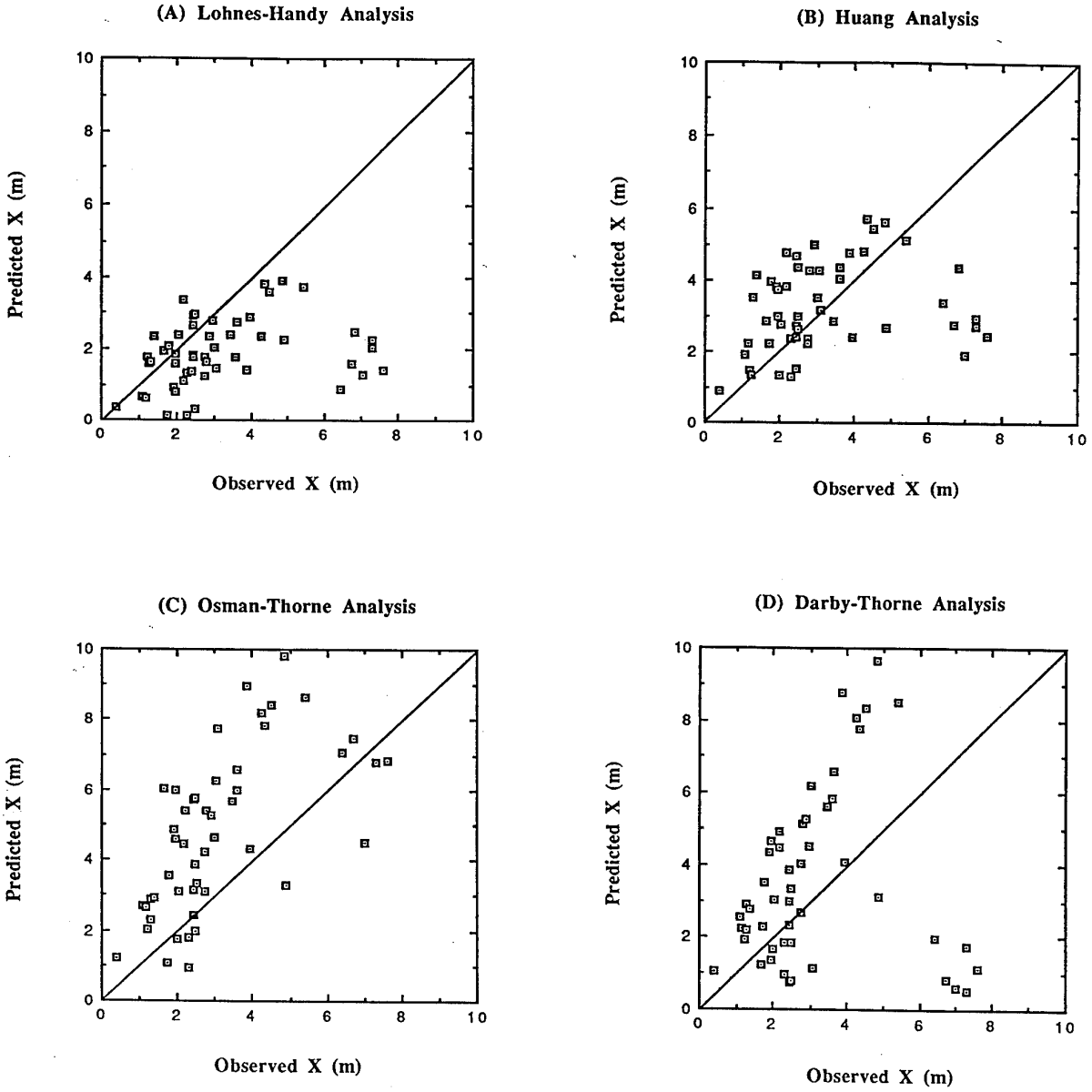

Figure 15 Comparison of predicted versus observed failure block width for (A) Lohnes-Handy, (B) Huang, (C) Osman-Thorne, and (D) Darby-Thorne bank stability analyses

Figure 13 shows that distinct differences arise in predictions of failure plane angle according to the methods of prediction. The Osman-Thorne and Darby-Thorne methods both employ a physically-based procedure to predict failure plane angle with relatively good, consistent, results though with a tendency to somewhat under-predict failure plane angle. This impression is confirmed by the calculated mean discrepancy ratios of 0.561 and 0.867 for the Osman-Thorne and Darby-Thorne analyses, respectively (Table 4). However, when the simple approximation based on bank and soil friction angles only is used to calculate failure plane angle, as is employed in both the Lohnes-Handy and Huang analyses, predictive ability decreases dramatically. Figure 13 clearly shows the poor predictive ability of these two analyses for failure plane angle, to an extent that is masked by the calculated mean discrepancy ratios for these analyses (Table 4). The mean discrepancy values of 1.237 (Lohnes-Handy) 1.281 (Huang) appear to suggest improved predictive ability relative to the Osman-Thorne analysis, but this is misleading. In fact predictions for these two analyses tend to be distributed equally badly either side of the correct values (Figure 13), forcing the mean discrepancy ratio closer to unity than is actually warranted. It is important to note that overall the Osman-Thorne and Darby-Thorne analyses tend to under-predict failure plane angle, which will tend to contribute to the over-prediction of factor of safety observed in the previous section. However, the Lohnes-Handy and Huang analyses tend to over-predict failure plane angle, suggesting that the cause of over-prediction of factor of safety for these analyses must be sought elsewhere. Of the tested analyses the Darby-Thorne analysis predicts incipient failure plane angles closest to the observed data.

Figure 14 illustrates that all of the analyses tend to give a large amount of scatter in predicted versus observed failure block volume values. The diagrams also suggest that while the Osman-Thorne and Darby-Thorne analyses tend to over-predict failure block volume, the Lohnes-Handy analysis tends to under-predict this parameter. The Huang analysis appears to give values which bisect the line of perfect agreement, but with a high degree of scatter. These qualitative impressions are confirmed by the calculated values of mean discrepancy ratio: Lohnes-Handy, 0.391; Huang, 1.030; Osman-Thorne, 2.586; and Darby-Thorne, 1.982, though the poor absolute deviation values (Table 4) indicate the high degree of scatter for all of these analyses. The magnitude of the volume of the failure block determines the weight of the block and, therefore, the predicted factor of safety. Over-predictions of failure block volume for the Osman-Thorne and Darby-Thorne analyses should tend to result in under-prediction of factor of safety (*i.e.* banks less stable than observed). That the opposite is in fact the case for both these analyses indicates that under-prediction of failure plane angle compensates for over-prediction of block volume in terms of its impact on factor of safety. Conversely, the over-prediction of failure plane angle for

the Lohnes-Handy and Huang analyses is compensated by under-prediction of failure block volume to the extent that factor of safety is also over-predicted by both these analyses. Indeed, the failure plane angle also directly influences the predicted block volume; lower angles leading to higher block volumes and *vice versa.* These results suggest that prediction of failure plane angle is critical in estimating the dimensions of the incipient failure block and the stability of the bank.

Figure 15 illustrates the predicted versus observed failure block widths obtained for each of the four analyses. Again, there appears to be a large amount of scatter in these relationships for all of the tested analyses, though there is a hint that the Osman-Thorne and Darby-Thorne analyses tend to cluster in a slightly more concentrated form. The scatter plots suggest that the Lohnes-Handy analysis tends to under-predict failure block width, while the Huang, Osman-Thorne and Darby-Thorne analyses all appear to over-predict this parameter. This impression is reflected in the calculated mean discrepancy ratios. In terms of ranking predictive ability for this parameter, the Huang analysis (1.249) appears to have the mean discrepancy ratio closest to unity, followed, in order, by Lohnes-Handy (0.703), Darby-Thorne (1.349) and Osman-Thorne (1.714). However, Figure 15 suggests that there is a tendency for the Darby-Thorne and Osman-Thorne to *systematically* over-predict failure block width which is not apparent in either of the other two analyses. The cause of the over-prediction for these two analyses is most likely the observed under-prediction of failure plane angle described previously.

Overall, it appears that the more consistent failure plane angle predictions of the Darby-Thorne and Osman-Thorne analyses enables these two analyses to provide superior predictions of incipient failure block geometry and, therefore, factor of safety when compared to the Lohnes-Handy and Huang analyses. It appears that the key to improving the predictive ability of the various bank stability analyses lies in more accurately estimating failure plane angle. In this regard, it is possible that the Darby-Thorne analysis would provide further improved predictions of failure plane angle if data were available for confining pressure and pore water pressure characteristics at the point of failure, as these variables also influence failure plane angle.

4.3.3 Critical Geometry: Darby-Thorne Analysis

In section 4.3.2, the ability of each of the four tested analyses to predict incipient failure block geometry was assessed. A feature of computer program based on the new analysis developed in this report is that it is able to estimate the critical geometry of initially stable banks by applying increments of lateral fluvial erosion and bed degradation to the initial, stable, bank profile, until critical conditions are reached. It is, therefore, possible to compare predictions of failure block geometry at critical conditions with the observed data

for the Darby-Thorne analysis. This is a useful exercise, since the failure block geometry at the point of failure determines the amounts of bank retreat, channel widening and volumes of sediment supplied to the channel once the banks become unstable. To determine the ability of the analysis to predict these parameters at critical conditions would provide insight into the utility of the analysis with respect to modelling channel width adjustments due to mass failure and bank erosion processes.

Table 5 Summary of calculated mean discrepancy ratio and absolute deviation of the discrepancy ratio for critical failure block geometry conditions using the Darby-Thorne bank stability analysis

Variable	*Me*	*Ad*
Failure Plane Angle, β	0.993	0.355
Failure Block Volume, *VB*	2.703	1.743
Failure Block Width, *x*	1.430	0.575
Flood-plain widening, *BW*	3.117	1.681

Critical geometry predictions were obtained for the Darby-Thorne analysis by running the analysis using observed bank geometries and "worst-case" soil properties. If the predicted factor of safety was less than 1.2, the failure block geometry so obtained was assumed to be the predicted critical failure block geometry. For predicted initial factors of safety greater than 1.2, the computer program based on this analysis was used to supply increments of lateral fluvial erosion and bed degradation until the critical conditions were obtained. For each analysis a $\frac{dW}{dZ}$ ratio of 0.1 was assumed. Predicted critical geometries so obtained were then compared with the observed data (Figure 16 and Table 5).

It can be seen that the critical failure block geometry parameters are predicted with varying degrees of accuracy. For failure plane angle, the calculated mean discrepancy ratio of 0.993 suggests relatively good predictive ability, but this impression is somewhat misleading. In fact, as Figure 16a indicates, there is considerable scatter about the "line of perfect agreement". When compared with the results obtained for the incipient geometry analysis, it seems that low failure plane angles tend to be raised during fluvial erosion, while the steeper failure plane angles tend to remain relatively constant, resulting in improved predictive ability overall, but with much increased levels of uncertainty for any one prediction. This tendency is as expected, since the steep failure planes probably correspond to critical banks, so that these banks would not be modified during the critical geometry analysis. Alternatively, fluvial erosion should act to heighten and steepen the

bank profile on the more stable banks, which in turn will steepen the predicted failure plane angle.

Failure block volumes are clearly significantly over-predicted, with a calculated mean discrepancy ratio of 2.703, though again the calculated absolute deviation of the discrepancy ratio and Figure 16b indicate that there is also a large amount of variation about the "line of perfect agreement". The increase in over-prediction of failure block volumes, compared to the incipient geometry analysis, corresponds to the increasing height of the failure block as degradation lowers the elevation of the toe of the bank.

There appears to be little difference in the failure block width parameters, x and BW, predicted by the incipient and critical geometry analyses, indicating that the shape of the critical block remains relatively constant during fluvial erosion. Thus, increasing failure plane angles tend to compensate for the increases in bank height, to maintain relatively constant block widths during fluvial erosion. It can be seen that total block width has a calculated mean discrepancy ratio of 1.430, compared to the flood-plain widening increment discrepancy ratio of 3.117. Both parameters indicate that the block width is significantly over-predicted by the Darby-Thorne analysis at critical conditions.

Overall, it appears that predictions of critical geometry obtained using the Darby-Thorne analysis do not compare well to the observed data. In particular, predictions of block magnitude (volume and width) are significantly over-predicted. This is an interesting result with regard to the potential for applying the new bank stability algorithm in the Darby-Thorne numerical channel evolution model. In that model, under-prediction of widening rates were attributed to under-prediction of failure block width and neglect of secondary failures (Darby *et al.*, In Review). Substituting the new bank stability analysis into the channel evolution model may well rectify this deficiency, but for the wrong reasons! It is clear that estimates of land loss and bank sediment yield obtained using this new analysis may be significantly in error.

On the other hand, these data in isolation can be somewhat misleading. It must be remembered that the Darby-Thorne analysis also over-predicts factor of safety, and that the over-prediction of critical failure block geometry parameters reflect the over-prediction of factor of safety. Moreover, estimates of land loss and bank sediment yield obtained using the Darby-Thorne analysis are a product not only of the magnitude of individual failures, but also the frequency at which those failures occur. The results presented in this report indicate that while the magnitude of block size will be over-predicted, the frequency of failures will be under-predicted by this analysis. The result of this counter-balancing effect may be that application of the Darby-Thorne bank stability analysis in analyses of long-term morphological response may well result in successful predictions, though it is recognised that this success would be for the wrong reasons. The important point is that it is clear that the Darby-Thorne analysis is the most physically-based, most widely applicable and by far

most successful in terms of predictive ability of the analyses tested here. For this reason, it is recommended that the bank stability analysis should be adopted in studies of long term river channel adjustments, such as the numerical channel evolution model developed by Darby and Thorne (In Review). This is now a topic of current research.

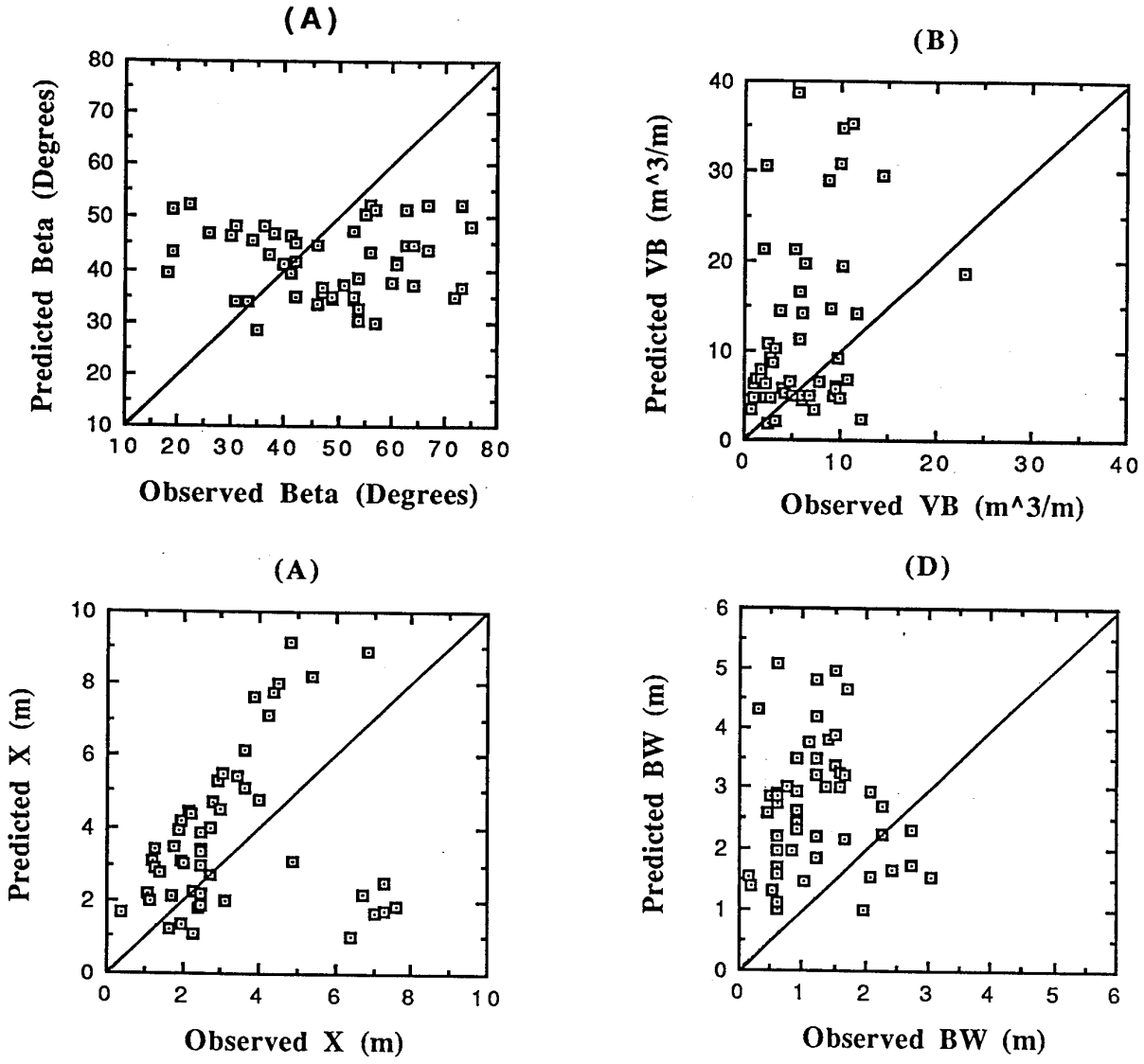

Figure 16 Predicted versus observed (A) Failure plane angles (B) Failure block volumes (C) Failure block widths and (D) Flood-plain widening increments obtained using the Darby-Thorne analysis for critical conditions

5. SUMMARY AND CONCLUSIONS

The ability to predict the stability and failure geometry of eroding riverbanks is an important pre-requisite for modelling numerically alluvial channel adjustments, as well as a requirement for predicting bank erosion rates and sediment yield associated with bank erosion. However, there are a number of limitations of existing bank stability analyses which limit their physical basis and predictive ability. Some of these limitations have been addressed here through the development of a new bank stability analysis. The new approach is applicable to steep, cohesive, non-layered riverbanks which fail along planar failure surfaces. The analysis is developed for banks with profiles characteristic of natural, eroding riverbanks. Failure plane angles are calculated using a physically-based approach; additionally the failure plane is not constrained to pass through the toe of the bank. Pore water and hydrostatic confining pressure effects are included in the analysis. Using the procedure developed by Darby (1994), the new analysis also is capable of predicting the probability of mass failure, as well as an overall factor of safety with respect to mass failure.

A new data set, comprising information about 51 individual mass-failures, has been used to compare the predictive abilities of 4 bank stability analyses: Lohnes and Handy (1968), Huang (1983), Osman and Thorne (1988) and the analysis developed in this report. Results indicate that the new analysis is the most successful of the tested analyses in terms of predicting the stability of riverbanks with respect to mass failure. However, the new analysis still significantly over-predicts bank stability. Nevertheless, it is demonstrated that the new analysis provides significant improvements to predictions of bank stability when compared to the other analyses. It is, therefore, concluded that application of the new analysis in the Darby-Thorne numerical channel evolution model (Darby, 1994; Darby and Thorne, In Review; Darby *et al.*, In Review) would result in improved quantitative predictions of channel adjustments. Implementation of the new bank stability analysis in the numerical channel morphology model is a topic of current research. It is recommended that the new analysis should also be used as a stand alone tool for analysis of bank stability and bank erosion problems.

The data set compiled to test the various bank stability analyses is also a resource of considerable value. The data set is supplied in spreadsheet format on a diskette with this report. The data set is the first suitable for testing the ability of bank stability analyses to predict accurately the factor of safety and geometry of individual observed mass-failures.

The new bank stability analysis may be used as a stand-alone analysis to aid engineers in the design of stable channels. To this end, the analysis has been developed as a computer program, which is supplied on diskette with this report, together with

supporting user documentation. The computer program may be used to calculate the factor of safety or probability of failure of riverbanks of geometry specified by the user. The user must specify the geotechnical characteristics of the bank material and select whether or not to include pore water and/or confining pressure effects in the analysis. If the user does select either these options he or she must specify the ground water surface elevation and elevation of the surface water in the channel, respectively.

A particular feature of the computer program is that it may be used to determine the amounts of fluvial erosion and bed degradation required to destabilize an initially stable bank to the point of failure. This feature allows the computer program to be utilised as a design aid in a variety of stable channel design applications, such as determining minimum grade-control structure elevations required to prevent degradation initiating channel widening and instability, or in estimating volumes of sediment supplied to the channel from fluvial erosion/bed degradation induced bank failures. It is concluded that the new analysis and computer program may be of use in aiding practicing engineers in a variety of problems which require analysis of bank erosion and width adjustments.

ACKNOWLEDGEMENTS

This research was supported by funding from the U. S. Army European Research Office, contract RND 7069-EN-01, which is gratefully acknowledged. The idea for this research developed from conversations with Andrew Simon of the United States Geological Survey, Raleigh, North Carolina, who also provided many valuable comments and suggestions during the course of this work. Thanks are also due to the continuing support of Mike Trawle and Ron Copeland at the United States Army Engineers Waterways Experiment Station, Vicksburg, Mississippi. Carlos Alonso and Earl Grissinger at the United States Department of Agriculture, Agricultural Research Service, National Sedimentation Laboratory at Oxford, Mississippi, provided the Goodwin Creek survey data set, which is also gratefully acknowledged. Bill Wolfe, United States Geological Survey (Nashville, Tennessee) and Bob Lohnes, Iowa State University, contributed valuable discussions about bank stability analyses in general and their bank stability models in particular.

Discussions with Jon Burgi, Colorado State University, led to helpful suggestions relating to the development of the computer program. In particular, some parts of the operation and data presentation of the computer program were inspired by his bank stability model BURGBANK. Nick Wallerstein, Department of Geography, University of Nottingham, provided valuable assistance and creative suggestions in the production and testing of the users-manual, which helped greatly to improve the quality and usability of the final product.

APPENDIX I. References

Darby, S. E. 1994. *A Physically-Based Numerical Model of River Channel Widening*, PhD Thesis Submitted to The University of Nottingham, England. p.276.

Darby, S. E. & Thorne, C. R. 1992. "Impact of channelization on the Mimmshall Brook, Hertfordshire, UK", *Regulated Rivers: Research & Management*, **7**, 193-204.

Darby, S. E. & Thorne, C. R. 1993. "Approaches to modelling width adjustment in curved alluvial channels", University of Nottingham, Department of Geography Working Paper **20**. p.90.

Darby, S. E. & Thorne, C. R. 1994. "Prediction of tension crack location and riverbank erosion hazards along destabilized channels", *Earth Surface Processes and Landforms*. **19**, 233-245.

Darby, S. E. & Thorne, C. R. In Review. "A physically-based numerical model of river channel evolution I: Development", *Journal of Hydraulic Engineering*.

Darby, S. E., Thorne, C. R. and Simon, Andrew. In Review. "A physically-based numerical model of river channel evolution I: Development", *Journal of Hydraulic Engineering*.

Huang, Y. H. 1983. *Stability Analysis of Earth Slopes*, Van Nostrand Reinhold, New York, p.305.

Johnson, P. A. 1992. "Reliability-based pier scour engineering", *Journal of Hydraulic Engineering*, **118**, 1344-1358.

Lohnes, R. & Handy, R. L. 1968. "Slope angles in friable loess", *Journal of Geology*, **76**, 247-258.

Lohnes, R. 1991. "A method for estimating land loss associated with stream channel degradation", *Engineering Geology*, **31**, 115-130.

Osman, A. M. & Thorne, C. R. 1988. "Riverbank stability analysis I: Theory", *Journal of Hydraulic Engineering*, **114**, 134-150.

Simon, Andrew. 1989. "A model of channel response in disturbed alluvial channels", *Earth Surface Processes and Landforms*, **14**, 11-26.

Simon, Andrew. 1992. "Energy, time, and channel evolution in catastrophically disturbed fluvial systems", *Geomorphology*, **5**, 345-372.

Simon, Andrew. & Hupp, C. R. 1986. "Channel widening characteristics and bank slope development along a reach of Cane Creek, West Tennessee", in Subitzky, Seymour (ed) *Selected papers in the hydrological sciences*, U. S Geological Survey Water-Supply Paper 2290, p113-126.

Simon, Andrew., Wolfe, W. J. & Molinas, A. 1991. "Mass wasting algorithms in an alluvial channel model", *Proceedings of the 5th Federal Interagency Sedimentation Conference*. Las Vegas, Vol. 2, p.8-22 to 8-29.

Spangler, M. G. & Handy, R. L. 1982. *Soil Engineering*, 4th Edition, Intext Educational, New York, N. Y, p.819.

Taylor, D. W. 1948. *Fundamentals of soil mechanics*, John Wiley & Sons, New York, p.700.

Thorne, C. R. 1982. "Processes and mechanisms of river bank erosion", in Hey, R. D., Bathurst, J. C. & Thorne, C. R. "*Gravel Bed Rivers* ", John Wiley & Sons, Chichester. 227-259.

Thorne, C. R. & Tovey, N. K. 1981. "Stability of composite river banks", *Earth Surface Processes and Landforms*, **6**, 469-484.

Thorne, C. R. & Osman, M. A. 1988. "The influence of bank stability on regime geometry of natural channels", in White, W. R. (ed) *International Conference on River Regime*, Hydraulics Research/John Wiley & Sons, Chichester. p135-147.

Thorne, C. R., Murphey, J. B. & Little, W. C. 1981. "Stream Channel Stability Appendix D: Bank stability and bank material properties in the bluffline streams of northwest Mississippi" *Report to US Army Corps of Engineers, Vicksburg District, Vicksburg, Mississippi.*

US Army Corps of Engineers. 1983. "Sacramento river and tributaries bank protection and erosion control investigation", California sediment studies, Sacramento District US Army Corps of Engineers.

Yalin, M. S. 1971. "On the formation of dunes and meanders", *Proceedings of the 14th International Congress of the Hydraulic Research Association, Paris,* 3, C13, 1-8.

APPENDIX II. List of Symbols

Ad = Absolute deviation of the discrepancy ratio

BW = Flood plain widening increment

BW^* = "Potential" flood plain widening increment

c = Soil cohesion

F_{cp} = Hydrostatic confining pressure

F_n = Function in equation (39)

F_n' = First derivative of function F_n

F_x = Horizontal component of F_{cp}

F_{x1} = Horizontal component of F_{cp} on lowest bank face

F_{x2} = Horizontal component of F_{cp} on middle bank face

F_{x3} = Horizontal component of F_{cp} on upper bank face

F_y = Vertical component of F_{cp}

FD = Driving force acting on incipient failure block

FR = Resisting force acting on incipient failure block

FS = factor of safety

g = gravitational acceleration

H = Total bank height

H' = Uneroded bank height

h_w = Effective head of ground water

i = Bank angle

K = Tension crack depth

K_h = Relic tension crack depth

L = Length of failure surface

Me = Mean of the discrepancy ratio

n = Number of items in data set

ΔT = Computational time step

U_w = Total pore pressure acting on failure plane

u_w = Pore pressure acting at a point on the failure plane

V = Volume of failure block per unit reach length

V_{ft} = Total volumetric bank material inflow flux due to mass failure

V_m = Reach-averaged total volumetric bank material inflow flux due to mass failure

W = Weight of water above bank face

W_t = Weight of incipient failure block

X = Function in equation (37)

X' = First derivative of X

X_o = Observed parameter

X_p = Predicted parameter

x = Total failure block width

x^* = Potential total failure block width

Δx = Model reach length

Y = Function in equation (38)

Y' = First derivative of Y

y_f = Elevation of base of failure plane

y_f^* = Dimensionless elevation of base of failure plane

y_{fp} = Elevation of flood plain

y_k = Elevation of base of tension crack

y_s = Elevation of base of uneroded bank slope

y_t = Elevation of base of relic tension crack

y_w = Surface water elevation

α = Angle between resultant of confining pressure and normal to failure plane

β = Failure plane angle

ϕ = Soil friction angle

γ = Soil unit weight

γ_w = Unit weight of water

ρ_w = Density of water

ω = Direction of resultant of confining pressure

ς = Effective head of surface water

APPENDIX III. Bank Geometry Database Users Manual

The bank geometry database used to test the predictive abilities of the selected bank stability analyses in this study is supplied on two 3.5" diskettes, labelled "Bank Geometry Database (Apple Format)" and "Bank Geometry Database (IBM Format)", respectively. The diskettes are formatted for Apple Macintosh and IBM compatible personal computers, as labelled. For the Apple Macintosh disk, data is presented in the form a Microsoft Excel (Version 3.0) spreadsheet package. The filename for the data base is "Geometry". For the IBM compatible disk, data is presented in the form a Lotus-1,2,3 (Version 4 for Windows) spreadsheet package. The filename for the data base is "Geometry".

It is strongly recommended that users make a back-up copy of the files containing the data base.

The database consists of bank geometry and soil property data for 51 separate mass failures located at sites along eroding creeks in northern Mississippi. The data is supplied on a spreadsheet so that users can easily utilise the data for their own purposes. Soil properties for "average" and "worst-case" conditions are also supplied. Data for each site is arranged in rows 6 to 56, inclusive, in the spreadsheet, with individual parameters containing the data items for each of these sites arranged in separate columns. These columns are arranged in the spreadsheet in the following way:

Column A. Location of Site. Text data in this column provides the name of the creek on which the site is located.

Column B. Data Source. Data in this column provides a reference to one of a number of footnotes at the base of the spreadsheet. These footnotes provide brief details concerning the source of the data for a site in the corresponding row.

Column C. Total Bank Height, H (m). Provides the value of the total bank height at observed critical conditions.

Column D. Uneroded Bank Height, H' (m). Provides the value of the uneroded bank height at observed critical conditions.

Column E. Bank Angle (Degrees). Provides the value of the uneroded bank slope at observed critical conditions.

Column F. Provides the tangent of the bank angle.

Column G. Provides the sine of the bank angle.

Column H. Provides the cosine of the bank angle.

Column I. Tension Crack Depth, K (m). Provides the value of the tension crack depth observed at critical conditions.

Column J. Relic Tension Crack Depth, K_h (m). Provides the value of the relic tension crack depth observed at critical conditions.

Column K. Failure Plane Angle, β (degrees). Provides the value of the failure surface angle observed at critical conditions.

Column L. Provides the tangent of the failure plane angle.

Column M. Provides the sine of the failure plane angle.

Column N. Provides the cosine of the failure plane angle.

Column O. Flood-Plain Widening Increment, BW (m). Provides the value of the flood-plain widening increment observed at the point of failure.

Column P. Total Failure Block Width, x (m). Provides the value of the failure block width observed at the point of failure.

Column Q. Failure Block Volume, VB (m^3m^{-1}). Provides the value of the unit volume of the failure block at the point of failure.

Column R. Blank Column.

Column S. Average Soil Unit Weight, γ (kNm^{-3}). Provides the value of the average, or "best case" soil unit weight. This corresponds to the measured value under "dry" conditions.

Column T. Average Soil Cohesion, c (kPa). Provides the value of the average, or "best case" soil cohesion. This corresponds to the measured value under "dry" conditions. The method of measurement is referenced in Column W.

Column U. Average Soil Friction Angle, ϕ (degrees). Provides the value of the average, or "best case" soil friction angle. This corresponds to the measured value under "dry" conditions. The method of measurement is referenced in Column W.

Column V. Provides the tangent of soil friction angle.

Column W. References the method of measurement of the soil properties. The characters in this column are cross-referenced with a foot note at the base of the spreadsheet.

Column X. Worst Case Soil Unit Weight, γ (kNm^{-3}). Provides the value of the "worst case" soil unit weight. This corresponds to the value estimated for "saturated" conditions.

Column Y. Worst Case Soil Cohesion, C (kPa). Provides the value of the "worst case" soil cohesion. This corresponds to the value estimated for "saturated" conditions. The method of measurement is referenced in **Column AB**.

Column Z. Worst Case Soil Friction Angle, ϕ (degrees). Provides the value of the "worst case" soil friction angle. This corresponds to the value estimated for "saturated" conditions. The method of measurement is referenced in **Column AB**.

Column AA. Provides the tangent of the "worst-case" soil friction angle.

Column AB. References the method of measurement of the soil properties. The characters in this column are cross-referenced with a foot note at the base of the spreadsheet.

Column AC. Blank Column.

Column AD. Total Pore Pressure, U_w (kPa). This data is unavailable.

Column AE. Confining Pressure, F_{cp} (kPa). This data is unavailable.

Column AF. Pore Pressure ratio, ru. This data is estimated for "worst case" conditions for saturated soils (see Huang, 1983).

Column AG. Location of Failure Plane, y_f*. This gives the dimensionless bank height (measured in an upwards direction from the base of the bank) at which the most critical failure surface is located.

APPENDIX IV. Bank Stability Model Users Manual

Requirements to Use the Computer Program

The source code of the computer model based on the bank stability analysis developed in this report is written in FORTRAN-77 and is contained on an MS-DOS formatted disk, labelled "Bank Program", along with an executable version of the code. This disk is supplied with original copies of this report. The disk also holds 4 example data files required to run the model: UNITWEIG.DAT, COHESION.DAT, FRICTION.DAT and SOILDATA.DAT. The source code is titled DARBY.FOR and the executable code is titled DARBY.EXE. To run the computer program, an IBM compatible PC with math co-processor installed is required. It is recommended that users should make back-up copies of the 6 files contained on the diskette, and load these files onto their PCs. It is recommended that the computer program and supporting data files should be installed in a single directory on the C: drive of the PC. Users may freely use the program supplied with this report, but may not distribute the code to other parties. The authors accept no responsibility or liability resulting from use of the computer program.

About the Manual

In this Appendix, details are provided which explain how to enter data to the model, how to select various user-specified options, and how to read the data stored in the output file. Worked examples, using the supplied example data files, are also presented to demonstrate the application of the computer program. In using this manual, it is assumed that the user has read and understood the main body of this report. Together, the report and manual provide sufficient information for users to train themselves to operate the computer program and apply it to analyse bank stability problems.

A. ENTERING DATA TO THE MODEL

The bank stability analysis developed in this report requires data relating to the geometry of the bank profile, the geotechnical properties of the bank soil, as well as information relating to the ground and surface water elevations. This data is supplied to the computer program in two ways. First, some data is stored in input data files, which must be edited prior to execution of the program. Second, data is supplied to the model directly, in response to a range of prompts that appear on the user's screen during model execution. It should be noted that all data is entered to the model in SI units, as described in the main

report. Reference should be made to the report if there is any doubt about the appropriate units to use for a particular input parameter.

1. Editing Input Data Files

It is necessary to check and edit a total of 4 input data files prior to running the computer program. The file UNITWEIG.DAT contains information about the frequency of occurrence of various values of soil unit weight for the analysed bank material. Similarly, the files FRICTION.DAT and COHESION.DAT contain information relating to the frequency of occurrence of the values of soil friction angle and cohesion, respectively, for the bank material. These three files are used to supply data required for the probabilistic bank stability analysis. The file SOILDATA.DAT contains summary information relating to the soil property frequency distributions contained in the previous three files. This file is used primarily, but not exclusively, to supply data required for the non-probabilistic bank stability analysis.

Between them these files contain all the information relating to the geotechnical properties of the bank soils necessary to execute the computer program. Users are warned that great care must be taken in editing the input data files. Care must be taken to ensure that not only are correct values entered for individual parameters, but that the data in each file is entered in the correct format. Also, certain constraints, in addition to those outlined in section 3.9 of the main report, exist on the range of values of some variables. These issues are now addressed in turn for each of the input data files.

UNITWEIG.DAT

This file contains data regarding the probability of occurrence of particular values of the soil unit weight. Data are entered in two columns. An example of the format of this file is provided in Table AIV1, which corresponds to the file UNITWEIG.DAT supplied on the diskette. The first column of numbers in the file represents the soil unit weight data, in the form of positive, non-zero values. Note that the soil unit weight values are entered in Nm^{-3}, not the more commonly used kNm^{-3}. The second column of numbers corresponds to the probability of occurrence (non-dimensional units) in the range ($0 \leq P(\gamma) \leq 1$) of each of the unit weight values. Since the second column denotes probabilities of occurrence, the values entered in this column must sum to a total of unity. Note that the first field is left blank (x denotes a blank field). Soil unit weight data entered in the first column then must occupy the next 7 fields, which includes one decimal place. Two fields are left blank to separate the first and second columns. The probability data in the second column must occupy the next

5 fields, including 3 decimal plates. Note that numeric characters must be entered into every field of both columns (*e.g.* 07000.0 must be entered, not 7000 or 7000.0).

Table AIV1 Example of format of UNITWEIG.DAT input data file

Field	1	2	3	4	5	6	7	8	9	0	1	2	3	4	5
	Blank	Soil Unit Weight Value (Nm^{-3})							Blank		Probability				
	x	0	7	0	0	0	.	0	x	x	0	.	0	0	0
	x	0	9	0	0	0	.	0	x	x	0	.	0	0	0
	x	1	1	0	0	0	.	0	x	x	0	.	0	0	0
	x	1	3	0	0	0	.	0	x	x	0	.	1	2	5
	x	1	5	0	0	0	.	0	x	x	0	.	0	6	2
	x	1	7	0	0	0	.	0	x	x	0	.	1	8	8
	x	1	9	0	0	0	.	0	x	x	0	.	6	2	5
	x	2	1	0	0	0	.	0	x	x	0	.	0	0	0
	x	2	3	0	0	0	.	0	x	x	0	.	0	0	0

Note that the total number of rows in the file is designated as a positive integer called NUM2. This integer is later required as input data in the file SOILDATA.DAT. In the above example NUM2 = 9. The maximum number of rows permitted is 59, so that the condition $1 \leq NUM2 \leq 59$ must be satisfied. The file UNITWEIG.DAT is not used in the non-probabilistic analysis. If it is intended to use only the non-probabilistic analysis, it is, therefore, not necessary to edit this file.

FRICTION.DAT

This file contains data regarding the probability of occurrence of particular values of the soil friction angle. Data are again entered in two columns. An example of the format of this file is illustrated in Table AIV2, which is the file FRICTION.DAT supplied on the disk with this report. The first column of numbers in the file represents soil friction angle data, in the form of positive, non-zero values. Soil friction angle values are entered in degrees. The second column of numbers corresponds to the probability of occurrence (non-dimensional units) in the range ($0 \leq P(\phi) \leq 1$) of the corresponding friction angle value. Since the second column denotes probabilities of occurrence, the values entered in this column should always sum to a total of unity. Note that the first field is left blank (x denotes a blank field). Soil friction angle data entered in the first column then must occupy the next 4 fields, which includes one decimal place. Two fields are left blank to separate the first and

second columns. The probability data in the second column must occupy the next 5 fields, including 3 decimal places. Note that numerical characters must be entered into every field of both columns (*e.g.* 07.5 is entered, not 7.5).

Table AIV2 Example of format of FRICTION.DAT input data file

Field	1	2	3	4	5	6	7	8	9	0	1	2
	Blank	Friction Angle (degs)				Blank		Probability				
	x	0	7	.	5	x	x	0	.	0	0	0
	x	1	2	.	5	x	x	0	.	0	6	3
	x	1	7	.	5	x	x	0	.	0	0	0
	x	2	2	.	5	x	x	0	.	1	2	5
	x	2	7	.	5	x	x	0	.	1	2	5
	x	3	2	.	5	x	x	0	.	3	7	5
	x	3	7	.	5	x	x	0	.	2	5	0
	x	4	2	.	5	x	x	0	.	0	6	2

Note that the total number of rows in the file is designated as a positive integer called NUM3. This integer is later required as input data in the file SOILDATA.DAT. In the above example NUM3 = 8. The maximum number of rows permitted is 59 (i.e. $1 \leq$ NUM3 ≤ 59). The file UNITWEIG.DAT is not used in the non-probabilistic analysis. If it is intended to use only the non-probabilistic analysis, it is, therefore, not necessary to edit this file.

COHESION.DAT

This file contains data regarding the probability of occurrence of particular values of the soil cohesion. Data are entered in two columns. An example of the format of this file is provided in Table AIV3, which corresponds to the file COHESION.DAT supplied on the diskette. The first column of numbers in the file represents the soil cohesion data, in the form of positive, non-zero values. Note that the soil cohesion values are entered in Nm^{-2}, not the more commonly used kNm^{-2}. The second column of numbers corresponds to the probability of occurrence (non-dimensional units) in the range ($0 \leq P(\gamma) \leq 1$) of each of the cohesion values. Since the second column denotes probabilities of occurrence, the values entered in this column must sum to a total of unity. Note that the first field is left blank (x denotes a blank field). Soil cohesion data entered in the first column then must occupy the next 7 fields, which includes one decimal place. Two fields are left blank to separate the

first and second columns. The probability data in the second column must occupy the next 5 fields, including 3 decimal plates. Note that numeric characters must be entered into every field of both columns (*e.g.* 02500.0 must be entered, not 2500 or 2500.0).

Table AIV3 Example of format of COHESION.DAT input data file

Field	1	2	3	4	5	6	7	8	9	0	1	2	3	4	5
	Blank	Soil Cohesion Value (Nm^{-2})							Blank		Probability				
	x	0	2	5	0	0	.	0	x	x	0	.	0	0	0
	x	0	7	5	0	0	.	0	x	x	0	.	1	8	7
	x	1	2	5	0	0	.	0	x	x	0	.	2	5	0
	x	1	7	5	0	0	.	0	x	x	0	.	4	3	8
	x	2	2	5	0	0	.	0	x	x	0	.	0	0	0
	x	2	7	5	0	0	.	0	x	x	0	.	0	0	0
	x	3	2	5	0	0	.	0	x	x	0	.	1	2	5
	x	3	7	5	0	0	.	0	x	x	0	.	0	0	0
	x	4	2	5	0	0	.	0	x	x	0	.	0	0	0

Note that the total number of rows in the file is designated as a positive integer called NUM4. This integer is later required as input data in the file SOILDATA.DAT. In the above example NUM4 = 9. The maximum number of rows permitted is 59, so that the condition $1 \leq NUM4 \leq 59$ must be satisfied. The file COHESION.DAT is not used in the non-probabilistic analysis. If it is intended to use only the non-probabilistic analysis, it is, therefore, not necessary to edit this file.

SOILDATA.DAT

This file contains the modal values of the soil cohesion, friction angle and unit weight frequency distributions, which are required to run the non-probabilistic bank stability analysis. If the frequency distributions are unavailable representative values of these soil parameters may be substituted for the modal values. In addition the file contains the integers NUM2, NUM3 and NUM4 which are used in the probabilistic bank stability analysis, and which refer to the number of rows entered in the UNITWEIG.DAT, FRICTION.DAT and COHESION.DAT data files, respectively. It is, therefore, necessary to check this input data file whichever bank stability analysis is selected.

Data is input to the file along 1 row in 6 columns, which occupy a variety of fields. An example of the format of this file is provided in Table AIV4, which corresponds to the

file SOILDATA.DAT supplied on the diskette. The first field is left blank. The first column of numeric characters represents the cohesion, entered in Pa. This column occupies 7 fields, of which 1 must be a decimal place. Two blank fields separate the first and second columns. Numeric characters in the second column represents the soil unit weight in Nm^{-3}. The second column also occupies 7 fields, of which 1 must be a decimal place. The second and third columns are separated by two blank fields. Numeric characters in the third column represents the soil friction angle, in degrees. This column occupies 4 fields, 1 of which must be a decimal place. Two blank fields separate the third and fourth columns. Numeric characters entered in the fourth column represents the integer NUM2. This value occupies 3 fields. Finally, the integers NUM3 and NUM4 occupy three fields each in the fifth and sixth columns, respectively. Again, these columns are separated by two blank fields.

Table AIV4 Example of format of SOILDATA.DAT input data file

x17500.0xx19000.0xx32.5xx009xx008xx009

WARNING

When entering data into the input data files, users are warned that great care must be taken to follow the procedures outlined above. In addition, as explained in the main report (see section 3.9), great care must be taken to specify realistically the soil property frequency distributions when applying the probabilistic bank stability analysis. Particular care must be paid in specifying soil unit weight distributions which have low magnitudes of soil unit weight with non-zero probabilities. When using the pore water pressure analysis, it is possible that some combinations of bank geometry and pore water pressure values, coupled with occurrence of low magnitude soil unit weight values, may lead to instances where computed failure block weights are less than computed pore water pressures. This is physically meaningless and spurious numerical results may, therefore, be obtained in those circumstances.

2. Entering Data at the Terminal

After editing the input data files, program execution commence by typing the name of the executable code, DARBY, and hitting the RETURN key. A sequence of prompts will appear requesting the user to input various data items. These data items can be sub-divided into a number of categories. These are now described in the order in which they appear on the screen.

2.1 Bank Geometry Data

Data prompts in this category request the various data which describe the shape of the bank profile (see the definition diagram Figure 4 in the main report). Users should note that all elevation data must be entered in metres, and should be input in absolute elevations (*e.g.* metres above sea level or other datum). In sequence, the following prompts appear:

"Enter flood-plain elevation (yfp)"

At this prompt, enter the elevation of the flood-plain (in metres), as defined by the point y_{fp} in Figure 4. Then hit the RETURN key to obtain the next prompt:

"Enter elevation of bank toe (yf)"

Type the elevation of the bank toe (in metres), as defined by the point y_f in Figure 4. Then hit the RETURN key to obtain the next prompt:

"Enter bank angle (degrees)"

Type the bank angle (in degrees), defined by the angle i in Figure 4. The value of the bank angle should be in the range $50 \leq i < 90$ to ensure computational integrity (see section 3.9 of main report). Then hit the RETURN key to obtain the next prompt:

"Enter elevation of base of bank slope (ys)"

Type the elevation of the base of the uneroded bank slope (in metres) defined by the point y_s in Figure 4. Note that if the bank is completely uneroded then $y_s = y_f$ should be used. Then hit the RETURN key to obtain the next prompt:

"Enter elevation of base of vertical slope (yt)"

Type the elevation (in metres) of the base of any relic tension crack that may be present, defined by the point y_t in Figure 4. If there is no tension crack present use $y_t = y_{fp}$. Then hit the RETURN key to obtain the next prompt:

"Enter elevation of base of tension crack (yk)"

Type the elevation (in metres) of the base of the tension crack (if present), defined by the point y_k in Figure 4. Users are reminded that values of tension crack depth greater than half the total bank height may lead to negative values of failure block weight, which is impossible. The computer program automatically constrains tension cracks so they do not exceed this maximum depth. This should be considered when interpreting analyses for which deeper cracks were (incorrectly) specified. If there is no tension crack present use $y_k = y_{fp}$. Then hit the RETURN key to obtain the next prompt, which is in the next category.

2.2 User-Specified Output File Name

The prompt:

"Please name the output data file"

requests the user to name the output data file to which the results of the analysis will be written. The user may use any combination of letters or numeric characters, up to a maximum of 10 characters. In addition to these 10 characters, the named output data file will automatically be given the extension _____.DAT. For example, if the user names the file "TEST1", the complete output file name will be named "TEST1.DAT". Users should not attempt to add this extension to their file name. After typing the file name, hitting the RETURN key obtains the next prompt.

2.3 Critical Geometry Analysis

The prompt

"Do you want to find the critical geometry (y/n)"

allows the user to select whether or not to analyse only the stability of the initially specified bank profile, or whether to use the program to estimate the amount of fluvial erosion required to bring that initially specified bank to the point of failure. If the critical geometry analysis is required, the user should type a lower-case "y" and hit the RETURN key, to obtain the next prompt. Typing any other key, including an upper-case "Y" will result in the critical geometry analysis *not* being selected. It is stressed that only a lower case "y" is permitted if the user wishes to select this analysis. It should also be noted that if this

analysis is selected, the user must also select the non-probabilistic bank stability analysis (see below). If the analysis is selected the next prompt:

"Enter bank erosion parameter (dW/dZ)"

allows the user to specify the ratio of lateral erosion to bed degradation supplied to the bank profile. In the absence of field data, it is suggested that the value of 0.1 may be entered as a reasonable default value for many cohesive riverbanks not subjected to severe particle-by-particle erosion. Hitting the RETURN key obtains the next prompt.

2.4 Ground Water Data

The next prompt allows the user to select whether or not to include pore water pressure effects in the bank stability analysis. In response to the prompt:

"Do you want to include pore pressure (y/n)"

the user should type a lower-case "y" and hit RETURN only if pore water pressure effects are to be included in the bank stability analysis. Typing any other key will result in the pore water pressure analysis not being selected. If the analysis is selected, the prompt:

"Enter ground-water surface elevation (gwse)"

requests the elevation (in metres) of the ground water surface, defined by the line GWSE in Figure 4. Any positive value in the range ($0 < \text{GWSE} \leq y_{fp}$) may be entered, though recall that analyses with values close to the flood-plain elevation may encounter difficulties for certain bank geometries and low values of soil unit weight (probabilistic analysis). Then hit the RETURN key to obtain the next prompt.

2.5 Surface Water Data

The next prompt allows the user to select whether or not to include hydrostatic confining pressure effects in the bank stability analysis. In response to the prompt:

"Do you want to include pore pressure (y/n)"

the user should type a lower-case "y" and hit RETURN only if hydrostatic confining pressure effects are to be included in the bank stability analysis. Typing any other key will

result in the confining pressure analysis not being selected. If the analysis is selected, the prompt:

"Enter surface water elevation (wse)"

requests the elevation (in metres) of the surface water surface, defined by the line WSE in Figure 4. Any positive value in the the range ($0 < WSE \leq y_{fp}$) may be entered. Then hit the RETURN key to obtain the next prompt.

2.6 Selection of Bank Stability Analysis

The prompt:

"Choose modal (np) or probabilistic (p) analysis"

allows the user to select between either of the non-probabilistic (modal) or probabilistic bank stability analyses. If the user has previously selected the critical geometry analysis, the user must select the non-probabilistic analysis at this point. To do this, the user should type lower-case "np" and hit the RETURN key. Typing any other key will select the probabilistic bank stability analysis. In either case, hitting RETURN obtains the next prompt.

Users should note that when the non-probabilistic analysis is selected, soil input data from the file SOILDATA.DAT is used. The probabilistic analysis utilises soil data from the COHESION.DAT, UNITWEIG.DAT and FRICTION.DAT files. The appropriate files should be checked carefully when interpreting the output data.

2.7 Data Check Prompt

The final prompt:

"Please check data and options (type ok to proceed)"

allows the user to check and, if necessary, correct the data input in response to the prompts. If no amendments are necessary, type lower-case "ok" and hit RETURN to continue program execution. If the user wishes to amend any user-specified data items, type any other key and hit RETURN. The data input process is then repeated from the first prompt. Note that file input data cannot be amended at this point. If an error is spotted in the input data files, it will be necessary to terminate program execution.

B. PROGRAM EXECUTION

After selecting the proceed option in response to the data check prompt, hitting the RETURN key results in continued program execution. Processing will continue until either:

1. A message is displayed indicating program termination. This indicates successful program execution. The user can now interpret the output data (see below).

2. A program-supplied diagnostic error message is displayed, followed by the termination message. The program-supplied diagnostic message will indicate the possible reason for program failure (see "error messages", below).

3. A compiler-supplied error message is displayed, followed by the termination message. Compiler-supplied error messages do not usually indicate the reason for failure, other than perhaps locating the point in the source code at which the program "crashed". In the unlikely event that such a failure occurs, it is recommended that the user should carefully check all input data. If this check fails to locate the reason for the error, contact the authors directly at the address on the cover of this report.

C. OUTPUT DATA

Once program execution is complete, output data is written to the file _____.DAT previously named by the user. To look at the output data, users must open their output file using an editor. In the file, data is presented in two sections; an input data summary and an output data summary. The input data summary describes the soil properties entered into the model, together with messages outlining the various options selected by the user. The soils data presented in the input data summary correspond to the modal soil values entered in the file SOILDATA.DAT. These values are used in the non-probabilistic bank stability analysis, but also serve to provide a summary of the representative soil properties specified in the probabilistic bank stability analysis. In interpreting the results, care should be taken that the modal soil values are accurately cross-referenced with the soil property frequency distributions.

The output data summary details the predicted stability of the specified bank, together with information about the geometry of the most-critical predicted failure surface. If the critical geometry analysis was selected, the degradation required to cause failure and the height of the critical bank is also displayed. Information is provided relating to the factor of safety (non-probabilistic analysis) or probability of failure (probabilistic analysis)

of the most critical bank. In the non-probabilistic analysis, the bank is predicted to be unstable with respect to mass failure if the factor of safety is less than or equal to unity. Bank stability increases as the factor of safety increases above unity, or as the probability of failure decreases. Output data relating to details of the geometry of the most critical failure surface, as defined in Figure 4, are then provided, for both types of analysis. In order, the output data summary lists the most critical failure plane angle, β (degrees), most critical failure block volume, VB (m^3/m), total failure block width, x, (m), flood-plain widening increment, BW (m) and dimensionless height of the most critical failure surface (y_f^*). This latter parameter is non-dimensionalized by dividing the height of the location of the most critical failure surface above the base of the bank by the total bank height. Thus a basal failure corresponds to $y_f^* = 0$.

D. ERROR MESSAGES

A number of program-supplied diagnostic error messages have been built into the program, to indicate probable reasons for program failure. These messages are now listed.

1. **Warning - pore water pressure options failed.** This message indicates that the program failed to select any of the possible solutions for pore water pressure. Check that realistic values of y_{fp}, y_f, y_s, y_k, y_t, GWSE and WSE have been selected.

2. **Warning - confining pressure option failed.** This message indicates that the program failed to select any of the possible solutions for hydrostatic confining pressure. Check that realistic values of y_{fp}, y_f, y_s, y_k, y_t, GWSE and WSE have been selected.

3. **Warning - failure plane options failed.** This message indicates that the program failed to select any of the possible solutions for failure plane angle. Check that realistic values of y_{fp}, y_f, y_s, y_k, y_t, GWSE and WSE have been selected.

4. **error - computed probability is more than 1.0.** This message indicates that the predicted probability of failure is greater than unity, which is incorrect. Check the soil property input data files for accuracy. Take particular care that the values NUM2, NUM3 and NUM4 are correctly entered in the SOILDATA.DAT file, and that the values of the probabilities entered in each of the UNITWEIG.DAT, FRICTION.DAT and COHESION.DAT files are realistic and sum to unity.

5. **error - computed probability is less than 0.0.** This message indicates that the predicted probability of failure is less than zero, which is incorrect. Check the soil property

input data files for accuracy. Take particular care that the values NUM2, NUM3 and NUM4 are correctly entered in the SOILDATA.DAT file, and that the values of the probabilities entered in each of the UNITWEIG.DAT, FRICTION.DAT and COHESION.DAT files are realistic and sum to unity.

6. **error - too much lateral erosion.** This message indicates that the value supplied for the fluvial erosion parameter results in so much lateral erosion that a vertical bank or undercut profile develops. Such a profile cannot be analysed by this model, but may be analysed using Thorne and Tovey (1981). Alternatively, try using a reduced value of dW/dZ.

7. **Type 1 Convergence failure at yf* = .** This warning message indicates that the failure plane angle iteration procedure failed to converge to a solution, for the failure surface at the indicated dimensionless bank height. If this occurs, the program sets the failure plane angle for that failure surface to the default value given by equation (40) in the main report, and computations continue: program execution, therefore, does not fail. If this warning message is displayed, users should however bear in mind the use of the default value in interpreting their output data.

8. **Type 2 Convergence failure at yf* = .** This warning message indicates that the failure plane angle iteration procedure converged to an unrealistic solution in which the failure plane angle was predicted to be negative, for the failure surface at the indicated dimensionless bank height. If this occurs, the program sets the failure plane angle for that failure surface to the default value given by equation (40) in the main report, and computations continue: program execution, therefore, does not fail. If this warning message is displayed, users should however bear in mind the use of the default value in interpreting their output data.

9. **Type 3 Convergence failure at yf* = .** This warning message indicates that the failure plane angle iteration procedure converged to an unrealistic solution in which the failure plane angle was predicted to be greater then the bank angle, for the failure surface at the indicated dimensionless bank height. If this occurs, the program sets the failure plane angle for that failure surface to the default value given by equation (40) in the main report, and computations continue: program execution, therefore, does not fail. If this warning message is displayed, users should however bear in mind the use of the default value in interpreting their output data.

E. TEST CASE

This check list example is provided to ensure that the user is familiar with the procedures used to run the model, and to check that the supplied program is working accurately. First load the example data files provided together with an executable version of the source code provided onto a computer. Then follow these steps:

1. Type DARBY and hit the RETURN key to initiate program execution.

2. In response to the prompts enter the following bank geometry values:

   i) Flood-plain elevation (yfp) = 4.0m
   ii) Elevation of bank toe (yf) = 1.5m
   iii) Bank angle = 65 degrees
   iv) Elevation of base of bank slope (ys) = 2.2m
   v) Elevation of base of vertical slope (yt) = 4.0m
   vi) Elevation of base of tension crack (yk) = 3.8m

3. Name the output data file.

4. Do not select the critical geometry, pore water pressure or confining pressure analyses.

5. Select the non-probabilistic bank stability analysis, check the data and type ok in response to the prompts.

6. Once program execution is complete, check the named output data file. If the user correctly specified the data and options, and the program is working correctly, the following output data should be obtained:

Factor of Safety	2.77
Failure Plane Angle (degrees)	52.39
Failure Block Volume (m^3/m)	1.40
Failure Block Width (m)	1.68
Flood-Plain Widening	.84
Height of Most Critical Failure Surface	.050

F. EXAMPLE APPLICATIONS

It is recommended that the user work through the following examples in order to become familiar with the potential applications of the model. Step-by step solutions to each problem are provided below, but users should attempt to work through the examples on their own prior to comparing their results with the given solutions. Each of the following examples are based on analysis of the bank profile shown in Figure AIV1. The corresponding bank material properties are summarized in Table AIV5. In the following examples, the user will apply the computer program to:

1. Determine the probability of failure of the bank described by Figure AIV1 and Table AIV5, without considering the effects of pore water pressure or hydrostatic confining pressure;
2. Determine the effects of including pore water pressure in the analysis of the stability of the bank, by analysing the probability of failure for the case of a ground water table at elevation 4.7m;
3. Determine the initial factor of safety of the bank described by Figure AIV1 and Table AIV5, and the amount of degradation required to erode the bank to the point of failure, assuming a fluvial erosion coefficient of 0.1. For simplicity, do not analyse pore water or hydrostatic confining pressure effects in this example.
4. Compare the amount of degradation required to bring the bank to failure when a ground water surface elevation of 4.7m is incorporated in the analysis, with the degradation amount determined in example (3). Again, assume the fluvial erosion coefficient has a value of 0.1, and exclude hydrostatic confining pressure effects.

Example 1: Solution

1. Enter the soil property data in Table AIV5 to the input files, UNITWEIG.DAT, COHESION.DAT and FRICTION.DAT. Enter the modal values of soil cohesion (14,000.0), friction angle (25.0) and unit weight (23,800.0) to the file SOILDATA.DAT, along with the values NUM2 (006), NUM3 (009), NUM4 (012).

2. Use the bank profile provided in Figure AIV1 to determine the values of y_{fp}, y_f, i, y_s, y_t and y_k. These should be, respectively, 6.0m, 2.0m, 70.0 degrees, 4.0m, 6.0m and 5.65m

3. Initiate program execution by typing DARBY and hitting the RETURN key.

4. Follow the prompts to enter the bank geometry data and name the output data file.

5. Do not select the critical geometry, pore water pressure or hydrostatic confining pressure options in this example.

6. Select the probabilistic bank stability analysis.

7. Check your input data and re-input the data or proceed, as applicable.

8. Wait for the program to complete execution. If the program successfully executes, go to the next step. Otherwise determine the cause of the program failure, and correct it by re-starting the procedure from step 1.

9. Open your named results file and read off the computed probability of failure. The correct solution is 0.645. If your answer does not agree with this value, check your input data carefully.

Example 2: Solution

1. Enter the soil property data in Table AIV5 to the input files, UNITWEIG.DAT, COHESION.DAT and FRICTION.DAT. The correct, formatted values entered in each of these files are the same as example 1. Enter the modal values of soil cohesion (14,000.0), friction angle (25.0) and unit weight (23,800.0) to the file SOILDATA.DAT, along with the values NUM2 (006), NUM3 (009), NUM4 (012).

2. Use the bank profile provided in Figure AIV1 to determine the values of y_{fp}, y_f, i, y_s, y_t and y_k. These should be, respectively, 6.0m, 2.0m, 70.0 degrees, 4.0m, 6.0m and 5.65m

3. Initiate program execution by typing DARBY and hitting the RETURN key.

4. Follow the prompts to enter the bank geometry data and name the output data file (Give a different name from that used for the first example).

5. Do not select the critical geometry, or hydrostatic confining pressure options in this example. However, do select the pore water pressure analysis and enter the ground water surface elevation, GWSE = 4.7m

6. Select the probabilistic bank stability analysis.

7. Check your input data and re-input the data or proceed, as applicable.

8. Wait for the program to complete execution. If the program successfully executes, go to the next step. Otherwise determine the cause of the program failure, and correct it by re-starting the procedure from step 1.

9. Open your named results file and read off the computed probability of failure. The correct solution should now be 0.692. If your answer does not agree with this value, check your input data carefully. Note that the probability of failure computed in this example compares to the value of computed in example 1. The effect of the including the pore water pressure arising from a ground water surface elevation of 4.7m is, therefore, to increase the probability of failure of the bank from 0.645 to 0.692.

Example 3: Solution

1. Enter the soil property data in Table AIV5 to the input files, UNITWEIG.DAT, COHESION.DAT and FRICTION.DAT. The correct, formatted values entered in each of these files are the same as example 1. Enter the modal values of soil cohesion (14,000.0), friction angle (25.0) and unit weight (23,800.0) to the file SOILDATA.DAT, along with the values NUM2 (006), NUM3 (009), NUM4 (012).

2. Use the bank profile provided in Figure AIV1 to determine the values of y_{fp}, y_f, i, y_s, y_t and y_k. These should be, respectively, 6.0m, 2.0m, 70.0 degrees, 4.0m, 6.0m and 5.65m

3. Initiate program execution by typing DARBY and hitting the RETURN key.

4. Follow the prompts to enter the bank geometry data and name the output data file.

5. Select the critical geometry analysis and enter the value of the fluvial erosion coefficient (dW/dZ = 0.1). Do not select the pore water pressure or hydrostatic confining pressure options in this example.

6. Select the non-probabilistic bank stability analysis.

7. Check your input data and re-input the data or proceed, as applicable.

8. Wait for the program to complete execution. If the program successfully executes, go to the next step. Otherwise determine the cause of the program failure, and correct it by re-starting the procedure from step 1.

9. Open your named results file and read off the initial factor of safety and amount of degradation required to initiate bank instability. The correct value of initial factor of safety is 1.03 - the bank is predicted to be on the verge of failure. The amount of degradation required to initiate failure is 0.10m. If your answers do not agree with these values, check your input data carefully.

Example 4: Solution

1. Enter the soil property data in Table AIV5 to the input files, UNITWEIG.DAT, COHESION.DAT and FRICTION.DAT. The correct, formatted values entered in each of these files are the same as example 1. Enter the modal values of soil cohesion (14,000.0), friction angle (25.0) and unit weight (23,800.0) to the file SOILDATA.DAT, along with the values NUM2 (006), NUM3 (009), NUM4 (012).

2. Use the bank profile provided in Figure AIV1 to determine the values of y_{fp}, y_f, i, y_s, y_t and y_k. These should be, respectively, 6.0m, 2.0m, 70.0 degrees, 4.0m, 6.0m and 5.65m

3. Initiate program execution by typing DARBY and hitting the RETURN key.

4. Follow the prompts to enter the bank geometry data and name the output data file.

5. Select the critical geometry analysis and enter the value of the fluvial erosion coefficient (dW/dZ = 0.1). This time, select the pore water pressure analysis and enter the ground water surface elevation value, GWSE = 4.7m. Do not select the hydrostatic confining pressure options in this example.

6. Select the non-probabilistic bank stability analysis.

7. Check your input data and re-input the data or proceed, as applicable.

8. Wait for the program to complete execution. If the program successfully executes, go to the next step. Otherwise determine the cause of the program failure, and correct it by re-starting the procedure from step 1.

9. Open your named results file and read off the initial factor of safety and amount of degradation required to initiate bank instability. The correct value of initial factor of safety is 0.92. The initial bank is, therefore, predicted to be unstable with respect to mass failure and no further degradation is required to initiate failure. If your answers do not agree with these values, check your input data carefully. Notice that the effect of including the pore water pressures resulting from insertion of the ground water table at 4.7m is to decrease the amount of degradation required to initiate failure from 0.10m to 0m, as compared to the value obtained in the third example. Notice also that the initial factor of safety value is also reduced, from 1.03 to 0.92.

Table AIV5 Summary of soil property values entered in input data files for example applications

UNITWEIG.DAT		COHESION.DAT		FRICTION.DAT	
Unit Weight	P(γ)	Cohesion	P(c)	F. Angle	P(ϕ)
20,200.0	0.000	10,000.0	0.000	10.0	0.100
21,600.0	0.150	11,000.0	0.000	15.0	0.100
23,800.0	0.494	12,000.0	0.100	20.0	0.200
24,900.0	0.206	13,000.0	0.150	25.0	0.200
26,210.0	0.150	14,000.0	0.220	30.0	0.200
30,000.0	0.000	15,000.0	0.160	35.0	0.100
		16,000.0	0.140	40.0	0.100
		17,000.0	0.120	45.0	0.000
		18,000.0	0.110	50.0	0.000
		19,000.0	0.000		
		20,000.0	0.000		
		21,000.0	0.000		

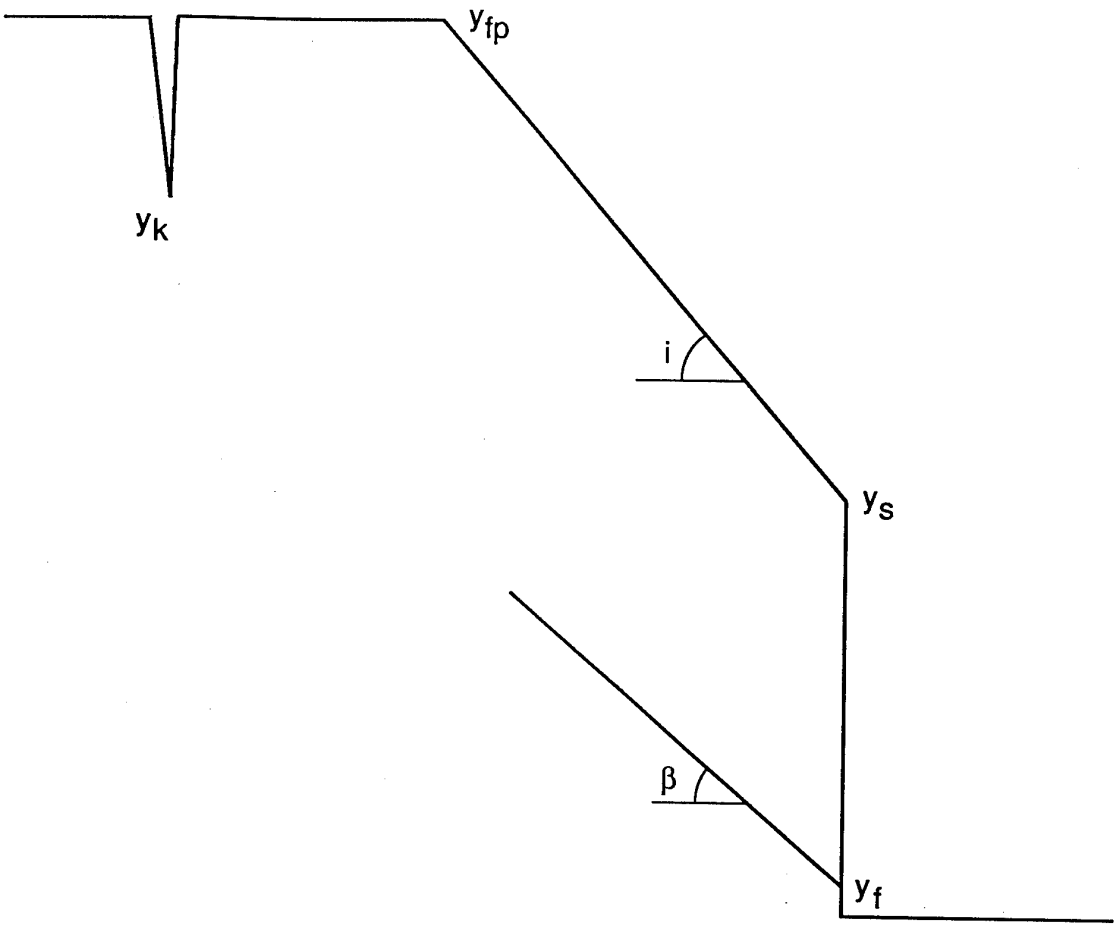

Figure AIV1 Definition diagram illustrating bank geometry parameters used in example applications